JEM Journal of Experimental Medicine

ARTICLE

Immunogenicity and efficacy of one and two doses of Ad26.COV2.S COVID vaccine in adult and aged NHP

Laura Solforosi[1*], Harmjan Kuipers[1*], Mandy Jongeneelen[1], Sietske K. Rosendahl Huber[1], Joan E.M. van der Lubbe[1], Liesbeth Dekking[1], Dominika N. Czapska-Casey[1], Ana Izquierdo Gil[1], Miranda R.M. Baert[1], Joke Drijver[1], Joost Vaneman[1], Ella van Huizen[1], Ying Choi[1], Jessica Vreugdenhil[1], Sanne Kroos[1], Adriaan H. de Wilde[1], Eleni Kourkouta[1], Jerome Custers[1], Remko van der Vlugt[1], Daniel Veldman[1], Jeroen Huizingh[1], Krisztian Kaszas[1], Tim J. Dalebout[2], Sebenzile K. Myeni[2], Marjolein Kikkert[2], Eric J. Snijder[2], Dan H. Barouch[3], Kinga P. Böszörményi[4], Marieke A. Stammes[4], Ivanela Kondova[4], Ernst J. Verschoor[4], Babs E. Verstrepen[4], Gerrit Koopman[4], Petra Mooij[4], Willy M.J.M. Bogers[4], Marjolein van Heerden[5], Leacky Muchene[1], Jeroen T.B.M. Tolboom[1], Ramon Roozendaal[1], Boerries Brandenburg[1], Hanneke Schuitemaker[1], Frank Wegmann[1], and Roland C. Zahn[1]

Safe and effective coronavirus disease–19 (COVID-19) vaccines are urgently needed to control the ongoing pandemic. While single-dose vaccine regimens would provide multiple advantages, two doses may improve the magnitude and durability of immunity and protective efficacy. We assessed one- and two-dose regimens of the Ad26.COV2.S vaccine candidate in adult and aged nonhuman primates (NHPs). A two-dose Ad26.COV2.S regimen induced higher peak binding and neutralizing antibody responses compared with a single dose. In one-dose regimens, neutralizing antibody responses were stable for at least 14 wk, providing an early indication of durability. Ad26.COV2.S induced humoral immunity and T helper cell (Th cell) 1–skewed cellular responses in aged NHPs that were comparable to those in adult animals. Aged Ad26.COV2.S-vaccinated animals challenged 3 mo after dose 1 with a SARS-CoV-2 spike G614 variant showed near complete lower and substantial upper respiratory tract protection for both regimens. Neutralization of variants of concern by NHP sera was reduced for B.1.351 lineages while maintained for the B.1.1.7 lineage independent of Ad26.COV2.S vaccine regimen.

Introduction

Development of multiple safe and effective vaccines to control the ongoing COVID-19 pandemic (Cucinotta and Vanelli, 2020; World Health Organization, 2020b) caused by severe acute respiratory syndrome coronavirus 2 (SARS-CoV-2; Wu et al., 2020; Zhu et al., 2020) is a global priority, and several vaccines have already been authorized or approved for use in humans to fight the pandemic (Voysey et al., 2021; Baden et al., 2021; Polack et al., 2020). Ideally, especially in the context of a pandemic, a vaccine provides both early onset of protection and durable protection. The durability of vaccine-elicited protection depends on the capacity of the vaccine platform, specific antigen (design), and vaccination regimen to efficiently stimulate the immune system (Cohen, 2019; Pulendran and Ahmed, 2011) and on several characteristics linked to the recipient of the vaccine (Zimmermann and Curtis, 2019). Age, for instance, plays an important role, as in the elderly the immune response to vaccines is usually reduced in magnitude and duration, potentially resulting in reduced vaccine efficacy (Wagner et al., 2018; Crooke et al., 2019; Gustafson et al., 2020; Weinberger, 2018). Although people of all ages are at risk of contracting COVID-19, the risk of developing severe or critical illness increases markedly with age (Mallapaty, 2020; Centers for Disease Control and Prevention, 2020), warranting the testing of COVID-19 vaccine candidates in different age cohorts.

The Ad26.COV2.S vaccine candidate is a replication-incompetent adenovirus 26 (Ad26)–based vector encoding the stabilized full-length SARS-CoV-2 spike protein based on the Wuhan-Hu-1 SARS-CoV-2 isolate and containing an aspartic acid (D) residue in amino acidic position 614 (D614; Bos et al., 2020). In preclinical efficacy studies, a single dose of Ad26.COV2.S provided robust protection against SARS-CoV-2 challenge (USA-WA1/2020 viral strain, D614) in both upper and lower

[1]Janssen Vaccines and Prevention B.V., Leiden, Netherlands; [2]Molecular Virology Laboratory, Department of Medical Microbiology, Leiden University Medical Center, Leiden, Netherlands; [3]Center for Virology and Vaccine Research, Beth Israel Deaconess Medical Center, Harvard Medical School, Boston, MA; [4]Biomedical Primate Research Centre, Rijswijk, Netherlands; [5]Non-Clinical Safety Toxicology/Pathology, Janssen Research and Development, Beerse, Belgium.

*L. Solforosi and H. Kuipers contributed equally to this paper; Correspondence to Roland C. Zahn: rzahn@its.jnj.com; S. Kroos's present address is Department of Rheumatology, Leiden University Medical Center, Leiden, Netherlands.

airways in rhesus macaques (Mercado et al., 2020) and protected Syrian golden hamsters from severe clinical disease (Tostanoski et al., 2020). Protective efficacy against SARS-CoV-2 in nonhuman primates (NHPs) in this and other studies strongly correlated with the presence of virus-binding and neutralizing antibodies in serum (Yu et al., 2020; Mercado et al., 2020; McMahan et al., 2021). These data corroborate previously reported findings on SARS-CoV showing that neutralizing antibody responses against the SARS-CoV spike protein, which binds to the same cellular receptor as SARS-CoV-2 for cell entry (Shan et al., 2020), were associated with protection against SARS-CoV challenge in nonclinical models (Chen et al., 2005).

Interim analyses of a Phase 1/2a study showed that Ad26.COV2.S elicits a prompt and robust immune response after a single-dose vaccination in both adults (18–55 yr old) and elderly (≥65 yr old) humans, as measured up to day 29 after immunization (Sadoff et al., 2021). Based on these data, the protective efficacy against COVID-19 is currently being evaluated in humans in a Phase 3 one-dose efficacy trial (ENSEMBLE trial, NCT04505722), for which a median follow-up of participants of 2 mo has shown an early indication of efficacy of 85% against severe/critical COVID-19 in humans (Ledford, 2021). Additionally, a second Phase 3 study (ENSEMBLE 2, NCT04614948) is currently evaluating vaccine efficacy and durability of a two-dose Ad26.COV2.S regimen as well, as the durability of immunity and efficacy may potentially be enhanced by a second dose. Indeed, in other programs with Ad26-based vaccines, two doses induced higher and more durable immune responses (Geisbert et al., 2011; Callendret et al., 2018; Salisch et al., 2019; Salisch et al., 2021). Here, we report immunogenicity and efficacy data after one- and two-dose regimens of Ad26.COV2.S in adult NHPs, including a group of aged NHPs, for a follow-up period up to 14 wk after the first vaccination. Protection was also studied in aged NHPs challenged with SARS-CoV-2 carrying a glycine residue in position 614 of the spike protein (D614G amino acid substitution), which emerged as the most prevalent SARS-CoV-2 spike variant (G614) in the global pandemic.

In addition, as new SARS-CoV-2 variants are rapidly emerging and spreading (Tegally et al., 2020 *Preprint*; European Centre for Disease Prevention and Control, 2020; World Health Organization, 2020a; Fontanet et al., 2021), we tested and report here the neutralizing capacity of sera from Ad26.COV2.S-immunized NHPs against the newly emerged SARS-CoV-2 spike variants from the B.1.1.7 and B.1.351 lineages that first emerged in the UK and Republic of South Africa (RSA), respectively.

Results

Immunogenicity of one- and two-dose Ad26.COV2.S vaccine regimens in adult rhesus macaques

Adult rhesus macaques (*Macaca mulatta*; 57 females and 3 males, 3.3–5.0 yr old) were immunized with either a single dose of 10^{11} viral particles (vp) or 5×10^{10} vp Ad26.COV2.S ($n = 14$ per group) or with two doses of 5×10^{10} vp Ad26.COV2.S with a 4- or 8-wk interval ($n = 14$ per group). A sham control group ($n = 4$) received an injection with saline at week 0 and week 8. SARS-CoV-2 spike protein–specific antibody responses were measured every 2 wk up to 14 wk after the first immunization by ELISA and pseudovirus neutralization assay (psVNA). The spike ELISA used for analysis of NHP samples is the same as that used for clinical samples (Sadoff et al., 2021). Immune responses were detected in all vaccinated animals as early as 2 wk after immunization and significantly increased for most animals by week 4 after immunization ($P \le 0.030$; paired *t* test; Fig. 1, A and B). Animals that received 10^{11} vp Ad26.COV2.S had 1.6-fold higher binding and 2.1-fold higher neutralizing antibody levels ($P = 0.008$ and $P = 0.004$, respectively; *t* test) relative to animals immunized with 5×10^{10} vp Ad26.COV2.S. Similar differences in response levels were maintained throughout the entire observation period. However, at week 14, neutralizing antibody titers were not statistically significantly different between the two one-dose groups ($P = 0.096$; paired *t* test). Spike protein–specific binding antibody levels declined more rapidly than neutralizing antibody levels, irrespective of the vaccine dose the animals had received.

A second vaccine dose given 4 or 8 wk after the first vaccination elicited a significant increase in spike protein–specific antibody responses relative to the predose 2 time point ($P \le 0.001$; ANOVA *t* test; Fig. 1, A and B). Compared with the one-dose regimen with 5×10^{10} vp Ad26.COV2.S, a second immunization given 4 or 8 wk after the first dose elicited a 5.7- and 11.8-fold increase ($P < 0.001$; ANOVA *t* test) in binding antibody concentrations and a 7.6- and 15.2-fold increase ($P < 0.001$; ANOVA *t* test) in neutralizing antibody titers, respectively, as measured 2 wk after dose 2. Similar differences between the one- and two-dose regimens were observed when comparing the antibody responses elicited by the two-dose 5×10^{10}–vp vaccine regimens with those elicited by the one-dose 10^{11}-vp vaccine dose.

While the two-dose vaccine regimens with 4- and 8-wk intervals elicited comparable spike protein–specific binding antibody concentrations 2 wk after the second immunization ($P = 0.456$; *t* test; Fig. 1 A), the geometric mean neutralizing antibody titer was 2.2-fold higher for the 8-wk regimen compared with the 4-wk regimen ($P = 0.005$; *t* test; Fig. 1 B). At week 4 and week 6 after second immunization, binding and neutralizing antibody levels declined in both two-dose groups, with similar kinetics maintaining the relative difference in neutralizing antibody titers (2.1- and 2.4-fold higher for the 8-wk regimen at 4 and 6 wk after second immunization, respectively; $P = 0.021$ and $P = 0.001$, respectively; *t* test).

In spite of the more rapid decline of binding antibody concentrations relative to neutralizing antibody titers in animals that received a one-dose regimen, we observed good overall correlation between binding and neutralizing antibody levels across time points for all tested regimens ($r_s = 0.7875$, $P < 0.001$; Spearman rank correlation). Correlation between binding and neutralizing antibody levels appeared particularly strong from week 6 onward, independent of the vaccine regimens the animals received (week 2 $r_s = 0.56$; week 4 $r_s = 0.64$; weeks 6–14 $r_s \ge 0.90$; $P < 0.001$; Spearman rank correlation; Fig. 1 C).

Immunogenicity of one- and two-dose Ad26.COV2.S vaccine regimens in aged rhesus macaques

As COVID-19 severity and mortality increase with age, we additionally analyzed the immunogenicity of Ad26.COV2.S in aged

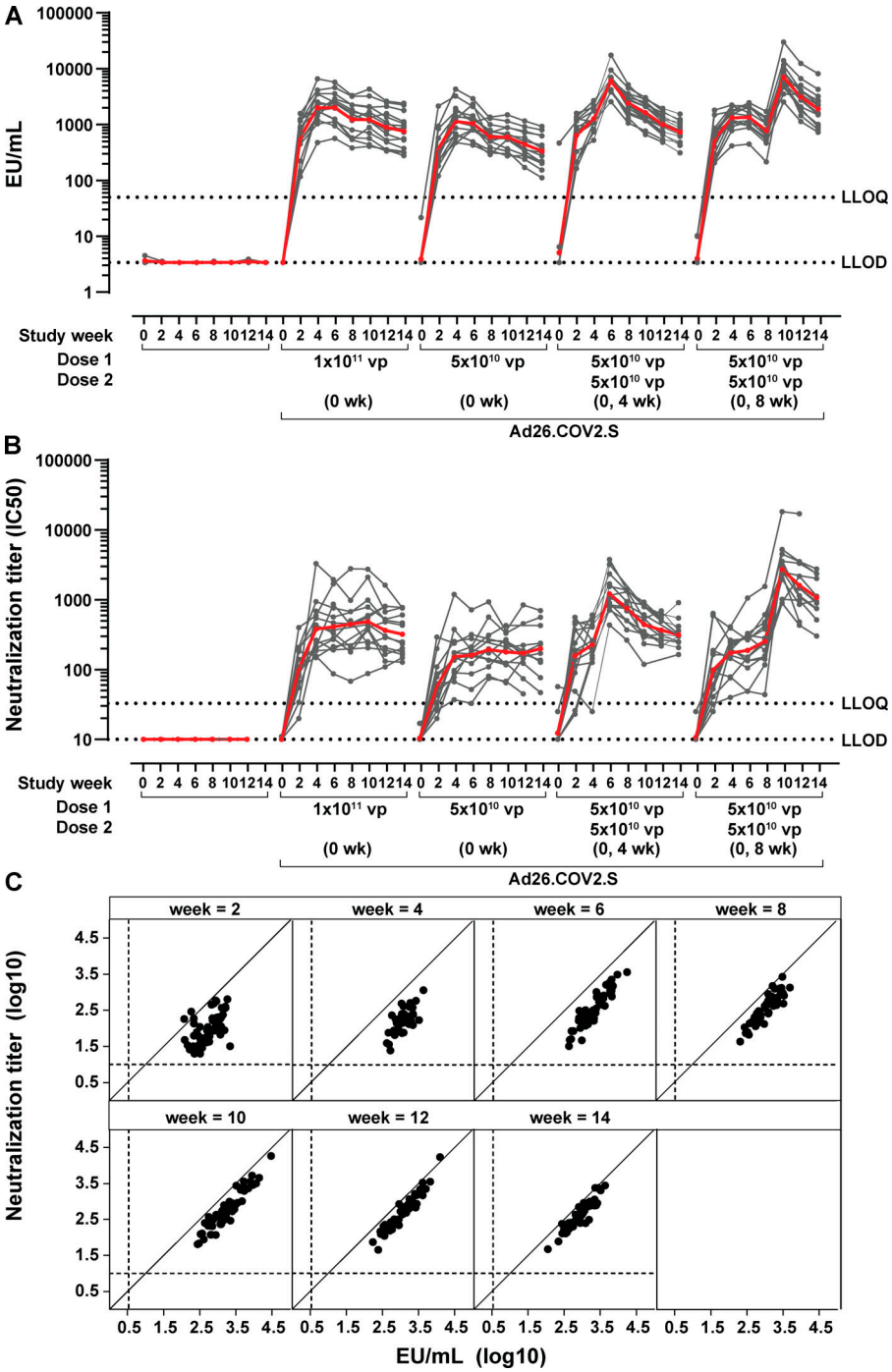

Figure 1. **SARS-CoV-2–specific humoral immune responses to one- and two-dose Ad26.COV2.S vaccine regimens in adult rhesus macaques. (A)** SARS-CoV-2 spike protein–binding antibody concentrations were measured over time in 480 NHP serum samples (60 NHPs and eight time points) with an ELISA qualified for human samples, using a trimeric, soluble, stabilized spike protein produced in mammalian cells as coating antigen. Antibody levels in the individual animals are depicted with gray points, and paired measurements are connected with gray lines. The geometric mean titer (GMT) of binding antibody responses per group is indicated with the red line. The dotted lines indicate the LLOD and LLOQ. **(B)** SARS-CoV-2 spike protein neutralizing antibody titers were measured over time in 456 NHP serum samples (60 NHPs and eight time points; 24 data points not available) with a psVNA qualified for human samples, using pseudotyped virus particles made from a modified VSVΔG backbone and bearing the S glycoprotein of SARS-CoV-2 Wuhan-Hu-1. Neutralizing antibody responses were expressed as the reciprocal of the sample dilution, where 50% neutralization is achieved (IC_{50}). Antibody levels in the individual animals are depicted with gray points, and paired measurements are connected with gray lines. The GMT of neutralizing antibody responses per group is indicated with the red line. The dotted lines indicate the LLOD and LLOQ. For binding and psVNA neutralizing antibody data, comparisons between specific vaccine groups were made with the two-sample *t* test in an ANOVA. Successive time points were compared using the paired *t* test per vaccine group. **(C)** Correlation between spike protein–specific binding antibody concentrations and neutralizing antibody titers per animal for all groups at each time point of analysis. The sham control group and week 0 (baseline) data were excluded. The dashed lines indicate the LLOD for each assay. Correlation coefficients between binding antibody concentrations and neutralizing antibody titers were calculated using two-sided Spearman rank correlation.

rhesus macaques (*M. mulatta*; 20 females, 13.8–21.9 yr old). An aluminum hydroxide ($Al(OH)_3$)–adjuvanted soluble trimeric spike protein stabilized in its prefusion conformation was included as a T helper type 2 cell (Th2 cell) skewing control vaccine for immunological assessment only. Groups were immunized with a one-dose regimen of 10^{11} vp Ad26.COV2.S (n = 6), a two-dose regimen of 5×10^{10} vp Ad26.COV2.S (n = 6), or a two-dose regimen of $Al(OH)_3$-adjuvanted 100 µg spike protein (n = 4), 8 wk apart. A sham control group received an Ad26 vector encoding an irrelevant antigen (Ad26.RSV.gLuc; sham control; n = 4) at week 0 and week 8. SARS-CoV-2 spike protein–specific binding and neutralizing antibody levels were measured every 2 wk up to 10 wk after the first immunization, and spike protein–specific cellular responses were measured at 4 and 10 wk.

Spike protein–specific binding antibody concentrations significantly increased for each vaccination regimen from week 2 onward ($P \le 0.034$; ANOVA paired *t* test comparing week 0 versus week 2). At weeks 6 and 8, the Ad26.COV2.S-induced antibody concentrations were significantly increased compared with $Al(OH)_3$-adjuvanted spike protein–induced concentrations ($P \le 0.036$; ANOVA *t* test). No statistically significant differences

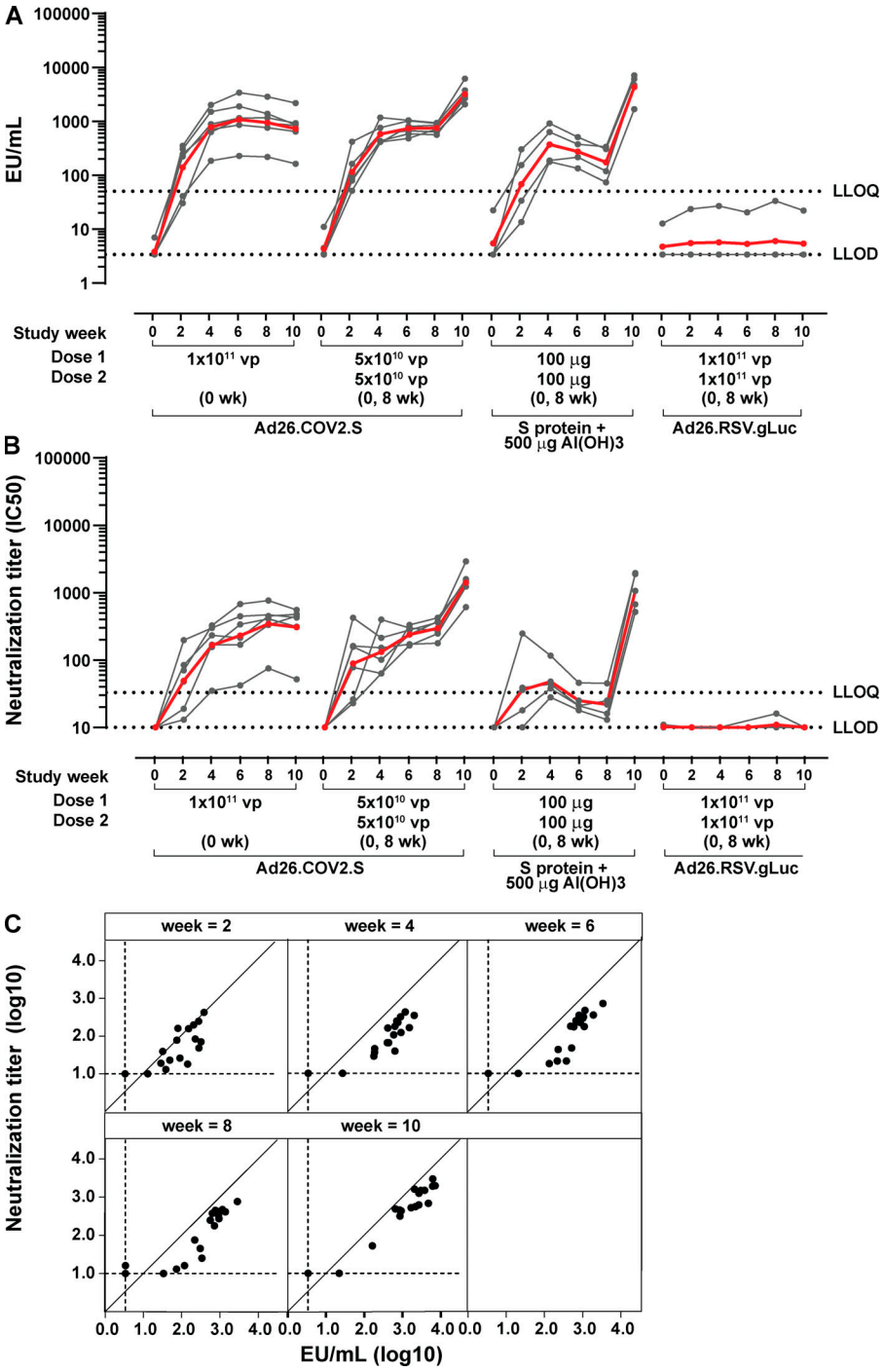

Figure 2. **SARS-CoV-2–specific humoral responses of one- and two-dose Ad26.COV2.S vaccine regimens in aged rhesus macaques. (A)** SARS-CoV-2 spike protein–binding antibody concentrations were measured over time in 120 NHP serum samples (20 NHPs and six time points) with an ELISA qualified for human samples using a trimeric, soluble, stabilized spike protein produced in mammalian cells as coating antigen. Antibody levels in the individual animals are depicted with gray points, and paired measurements are connected with gray lines. The geometric mean titer (GMT) of binding antibody responses per group is indicated with the red line. The dotted lines indicate the LLOD and LLOQ. **(B)** SARS-CoV-2 spike protein neutralizing antibody titers were measured over time in 116 NHP serum samples (20 NHPs and six time points; four data points not available) with a psVNA qualified for human samples using pseudotyped virus particles made from a modified VSVΔG backbone and bearing the S glycoprotein of SARS-CoV-2 Wuhan-Hu-1. Neutralizing antibody responses were expressed as the reciprocal of the sample dilution where 50% neutralization is achieved (IC_{50}). Antibody levels in the individual animals are depicted with gray points, and paired measurements are connected with gray lines. The GMT of neutralizing antibody responses per group is indicated with the red line. The dotted lines indicate the LLOD and LLOQ. For binding and psVNA neutralizing antibody data, comparisons between specific vaccine groups were made with the two-sample *t* test in an ANOVA. Successive time points were compared using the paired *t* test per vaccine group. **(C)** Correlation between spike-specific–binding antibody concentrations and neutralizing antibody titers per animal for all groups at each time point of analysis. The sham control group and week 0 (baseline) data were excluded. The dashed lines indicate the LLOD for each assay. Correlation coefficients between binding antibody concentrations and neutralizing antibody titers were calculated using two-sided Spearman rank correlation.

in antibody responses elicited by the two regimens using different Ad26.COV2.S dose levels could be detected up to week 8. At week 10, 2 wk after the second dose, the groups that received a second dose of 5×10^{10} vp Ad26.COV2.S or $Al(OH)_3$-adjuvanted spike protein had significantly higher antibody concentrations compared with recipients of the single-dose 10^{11} vp Ad26.COV2.S (4.4-fold and 5.9-fold for the 5×10^{10}–vp Ad26.COV2.S group and $Al(OH)_3$-adjuvanted spike protein group, respectively; $P \leq 0.002$; ANOVA *t* test). Spike-specific antibody concentrations between the two-dose regimens were not significantly different ($P = 0.482$; Fig. 2 A).

In aged animals, a single dose of 10^{11} vp Ad26.COV2.S induced neutralizing antibody titers at week 2, which significantly increased between 1.4- and 4.9-fold compared with the previous time point until week 8 ($P \leq 0.015$; Tobit ANOVA z-test) and remained stable thereafter up to week 10. Similarly, the two-dose 5×10^{10}–vp Ad26.COV2.S regimen induced neutralizing antibody titers that significantly increased 1.8- and 1.2-fold compared with previous time points from week 4 onward up to week 8 ($P \leq 0.023$; Tobit ANOVA z-test). At week 10, 2 wk after the second dose, antibody titers were increased 4.7-fold compared with week 8 ($P < 0.001$; Tobit ANOVA z-test), independent

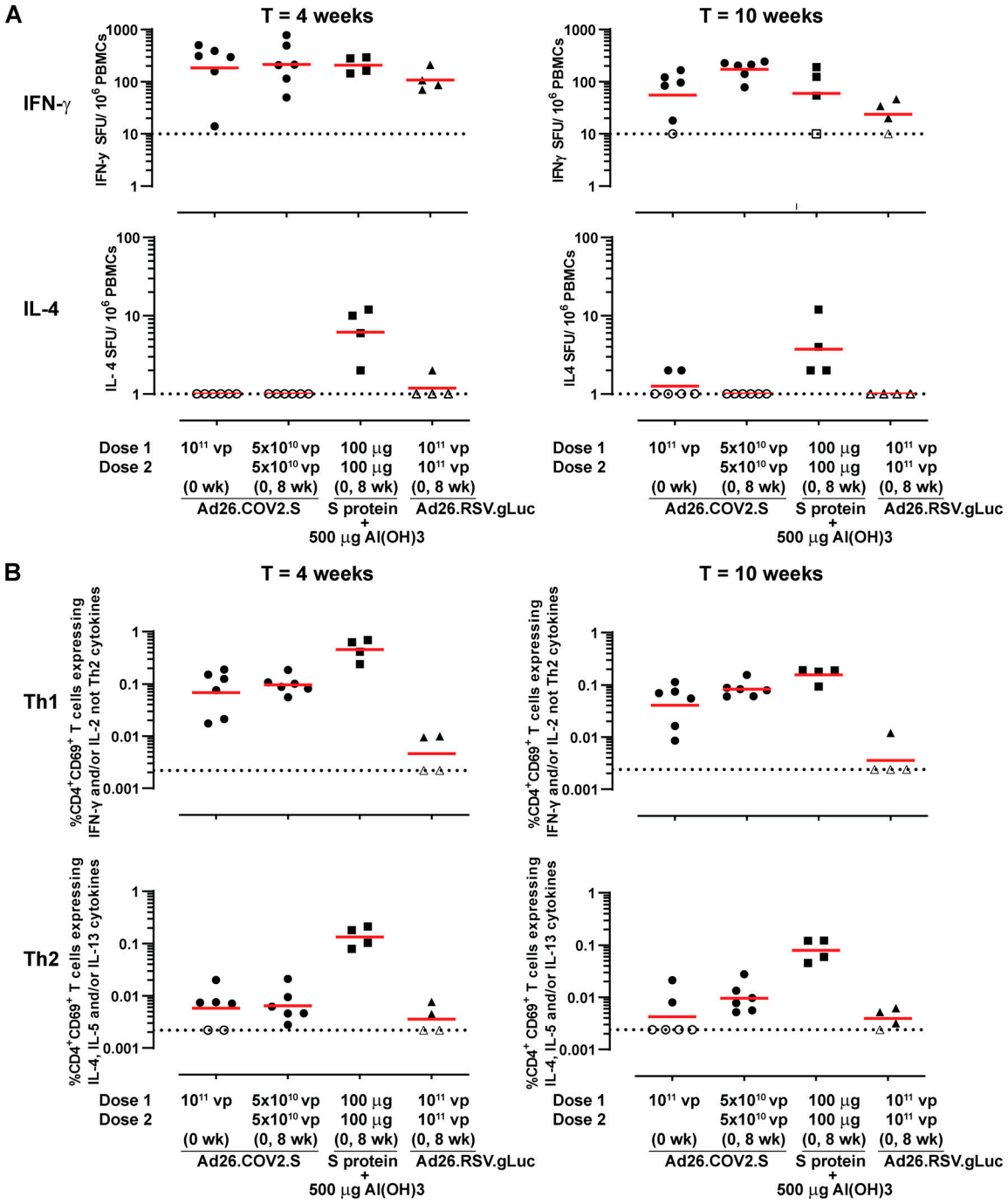

Figure 3. **SARS-CoV-2–specific cellular immune responses after vaccination of aged rhesus macaques. (A)** Spike protein–specific T cell responses as measured in 40 NHP PBMC samples (20 NHPs and two time points) with an IFN-γ/IL-4 double-color ELISPOT at indicated time points. The geometric mean titer (GMT) response per group is indicated with a horizontal line. Samples with background subtracted counts below or equal to zero were set at 10 and 1 for IFN-γ and IL-4, respectively, for visualization purposes and are indicated by open symbols and the dotted line. **(B)** Spike protein–specific Th1 and Th2 cell responses as measured in 40 NHP PBMC samples (20 NHPs and two time points) by ICS at indicated time points. Frequency of $CD4^+CD69^+$ T cell–expressing Th1 cytokines (IFN-γ and/or IL-2 and not IL-4, IL-5, and IL-13) or Th2 cytokines (IL-4 and/or IL-5 and/or IL-13). SFU, spot-forming units. The geometric mean response per group is indicated with a horizontal line. The dotted line indicates the technical threshold. Open symbols denote samples at technical threshold.

of the presence of Ad26 neutralizing antibody titers resulting from the first vaccine dose (Fig. S1). $Al(OH)_3$-adjuvanted spike protein induced only low and transient levels of neutralizing antibodies above the lower limit of quantification (LLOQ) after the first dose in two out of four animals only. At week 10, however, 2 wk after the second dose, neutralizing antibody titers increased 4.8-fold compared with week 8, in the same range as the Ad26.COV2.S groups ($P < 0.001$; Tobit ANOVA z-test). Pairwise comparison of vaccine groups at week 10 showed that the two-dose 5×10^{10}–vp Ad26.COV2.S regimen

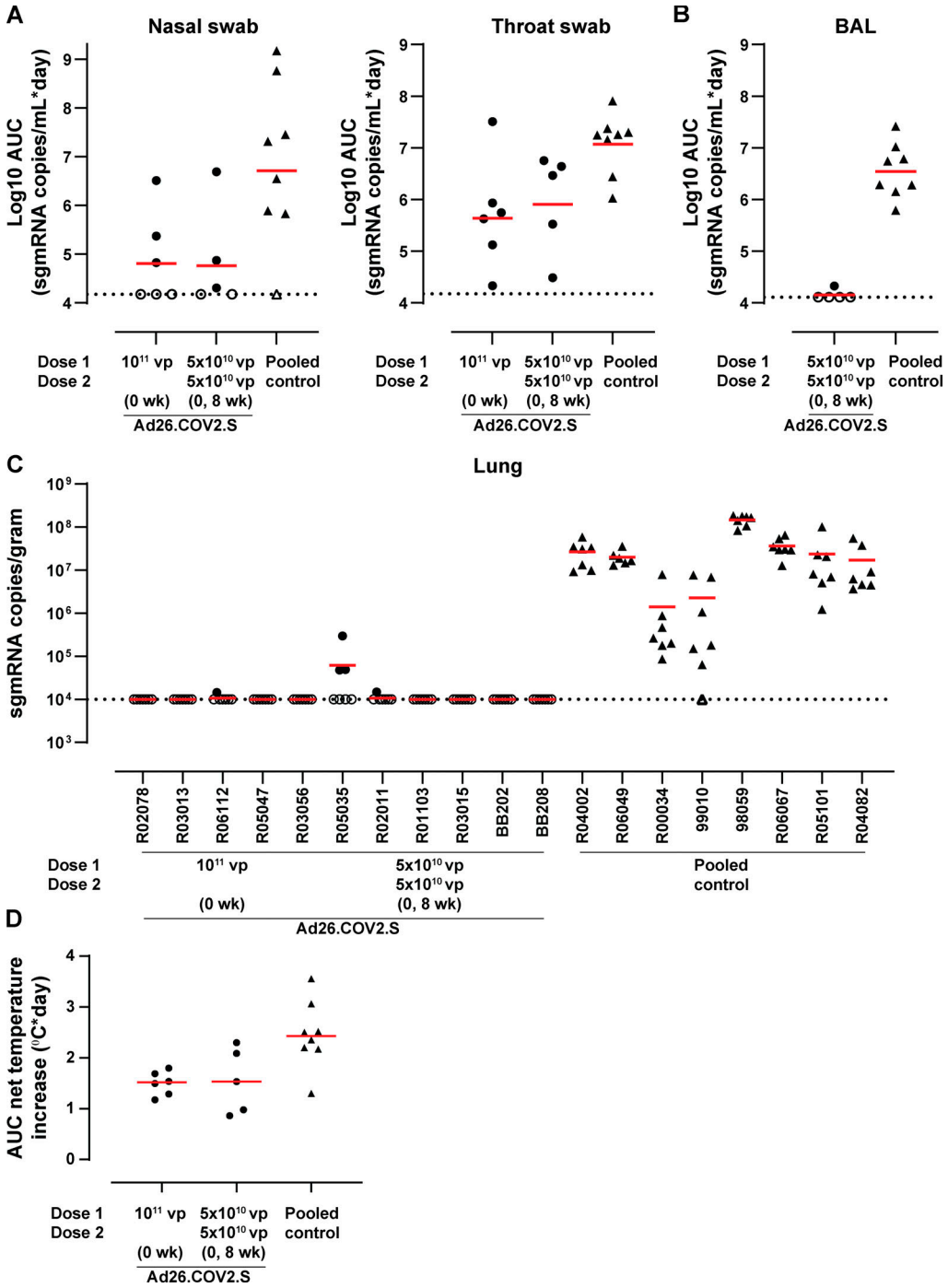

Figure 4. **Protective efficacy against SARS-CoV-2 inoculation after vaccination of aged rhesus macaques. (A–D)** Animals were challenged with 10^5 $TCID_{50}$ SARS-CoV-2 administered intranasally and intratracheally 13 wk after the first vaccine dose. Data from a challenge of naive animals (n = 4) using an identical challenge strain, challenge regimen, and readouts were added to the sham control group data, collectively referred to as pooled control, to increase statistical power. **(A)** Cumulative viral load (sgmRNA) in daily nasal (left panel) and tracheal (right panel) swabs, defined by AUC calculation and expressed as log_{10} AUC (sgmRNA copies/ml × days) from 19 NHPs. Note that for AUC calculation, the day of death of all animals was aligned to day 7 to allow combining data from animals euthanized at day 7 and day 8. **(B)** Cumulative viral load (sgmRNA) in BAL, obtained every other day during the follow-up period, defined by AUC calculation and expressed as log_{10} AUC (sgmRNA copies/ml × days) from 13 NHPs. Note that it was only possible to perform BAL on a limited number of animals, and it was decided to exclude the one-dose 10^{11}-vp Ad26.COV2.S group. **(C)** Viral load (sgmRNA) in lung tissue. Viral load was measured in each individual lung lobe (seven) of each animal (19 NHPs) and expressed as log_{10} sgmRNA copies/gram. A lower right lung lobe sample of one animal in the pooled control group was not available. **(D)** Fever duration, defined as AUC of the net temperature increase for each animal (19 NHPs) during the first 6 consecutive d of the follow-up period relative to a prechallenge baseline period. Red horizontal lines represent group geometric means; the dashed horizontal line indicates the LLOQ. Open symbols denote samples at LLOQ. Mean nasal and trachea swabs and BAL AUC values of each group were pairwise compared using Tobit ANOVA with post hoc z-test. Mean net temperature difference AUCs were pairwise compared between groups by t test.

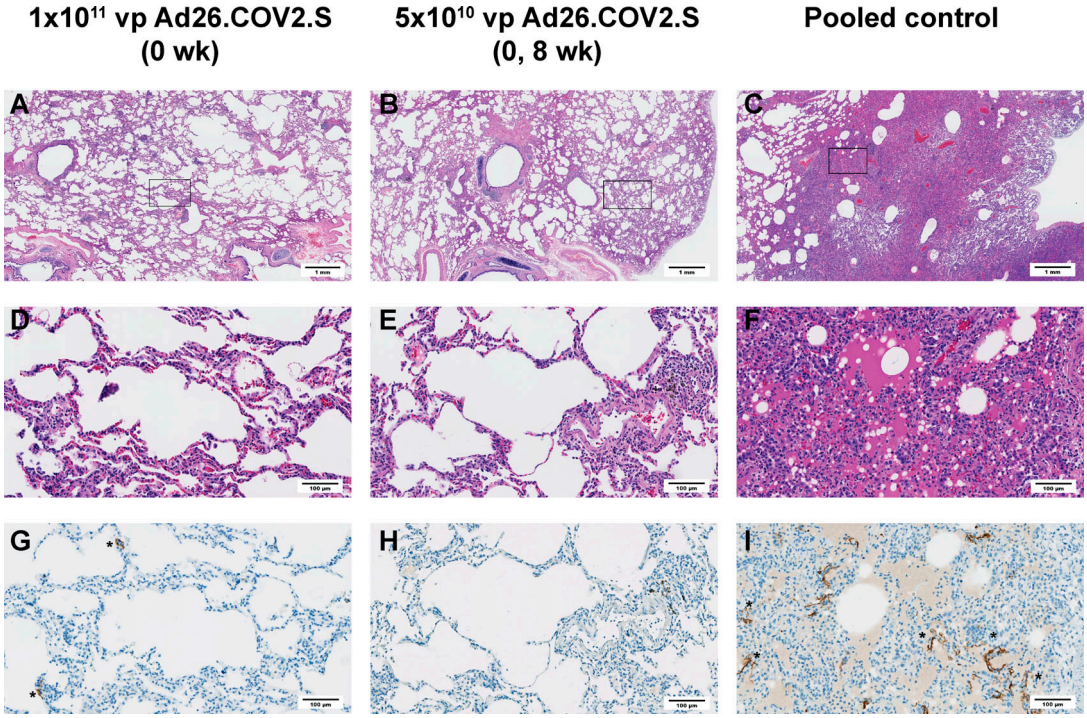

Figure 5. **Lung histology after SARS-CoV-2 inoculation of vaccinated aged rhesus macaques**. Seven individual lung lobes were evaluated for each animal in each treatment group (19 NHPs total). **(A–C)** 20× magnification overview image per treatment group. Scale bar is 1 mm. **(D–F)** H&E staining of rectangular areas as indicated in A–C. **(D)** In the one-dose 10^{11}-vp Ad26.COV2.S group, minimal mononuclear cell interstitial infiltrate and minimal perivascular cuffing was observed. **(E)** In the two-dose 5 × 10^{10}–vp Ad26.COV2.S group, multifocal small areas with minimal mixed-cell interstitial infiltrates (macrophages, scattered neutrophils, and lymphocytes) and minimal perivascular cuffing were observed. Alveolar lumina contained minimal macrophages, lymphocytes, and scattered neutrophils. **(F)** In the pooled control group animals, here represented by an animal of the Ad26.RSV.gLuc sham control group, focally extensive to diffuse lesions were observed with moderate mononuclear cell infiltrate in interstitium (macrophages, lymphocytes) and mild type II pneumocyte hyperplasia. Alveolar lumina contained edema, macrophages, lymphocytes, and scattered neutrophils. **(G–I)** SARS-CoV-2 –N immunohistochemistry (brown staining) of rectangular areas as indicated in A–C. Antigen-positive pneumocytes are marked with an asterisk (*). In the one-dose 10^{11}–vp Ad26.COV2.S group, only one out of six animals had a single lung lobe in which antigen-positive pneumocyte staining was observed. **(G)** Focal area with individual SARS-CoV-2 N-positive pneumocytes (*) in the left caudal lung lobe. **(H)** Absence of SARS-CoV-2 N-positive pneumocytes in all lung lobes from all animals in the two-dose 5 × 10^{10}–vp Ad26.COV2.S group. **(I)** Multifocal minimal to moderate numbers of SARS-CoV-2 N-positive pneumocytes (*) in seven out of eight pooled control animals. D–I are 200× magnification; scale bar is 100 µm.

or $Al(OH)_3$-adjuvanted spike protein induced significantly higher neutralizing antibody titers compared with the single-dose 10^{11}-vp Ad26.COV2.S group (4.9- and 3.5-fold for 5 × 10^{10}–vp Ad26.COV2.S and $Al(OH)_3$-adjuvanted spike protein groups, respectively; $P \leq 0.003$; Tobit ANOVA z-test). Neutralizing antibody titers were not significantly different ($P = 0.508$; Tobit ANOVA z-test) between the two-dose regimens at week 10 (Fig. 2 B). The spike protein–specific neutralizing antibody titers strongly correlated with binding antibody concentrations ($r_s = 0.93$, $P < 0.001$; Spearman rank correlation across all groups and time points, except week 0), showing the higher sensitivity of the ELISA. This correlation was rather uniform at all time points (r_s between 0.82 and 0.94, $P < 0.001$; Spearman rank correlation across all groups, per time point; Fig. 2 C). There was also a strong correlation observed between neutralizing antibody titers as measured in the psVNA and in the two assays performed with wild-type SARS-CoV-2 virus using a D614G isolate (Leiden-0008; $r_s = 0.90$, $P < 0.001$; Spearman rank correlation; Fig. S2 A) and the D614 Victoria/1/2020 isolate ($r_s = 0.91$, $P < 0.001$; Spearman rank correlation; Fig. S2 B).

Spike protein–specific T cell responses were measured with ELISPOT assay and intracellular cytokine staining (ICS) using peripheral blood mononuclear cells (PBMCs) stimulated with 15-mer peptides overlapping by 11 amino acids and spanning the complete SARS-CoV-2 spike protein. Both Ad26.COV2.S regimens as well as $Al(OH)_3$-adjuvanted spike protein induced IFN-γ responses as measured by ELISPOT at 4 wk after the first dose. At week 10, IFN-γ responses were lower for the 10^{11}-vp Ad26.COV2.S and adjuvanted spike protein groups compared with week 4. In animals vaccinated with the two-dose 5 × 10^{10}–vp Ad26.COV2.S regimen, IFN-γ responses at week 10 were comparable to week 4, suggesting that a second dose of Ad26.COV2.S maintains spike-specific T cell responses. Substantial IL-4 responses were observed only for the $Al(OH)_3$-adjuvanted spike protein group at both week 4 and week 10 by ELISPOT (Fig. 3 A). Of note, IFN-γ responses were detected in the control group as well, possibly due to the presence of non–T cells producing IFN-γ.

$CD4^+$ and $CD8^+$ T cell cytokine responses were also analyzed by ICS. Ad26.COV2.S induced a $CD4^+$ Th1-biased response with minimal expression of Th2 cytokines, while $Al(OH)_3$-adjuvanted spike protein induced a more dominant Th2 response (Fig. 3 B and Fig. S3 A). Spike protein–specific $CD8^+$ T cells induced by Ad26.COV2.S mainly produced IFN-γ and IL-2, while $CD8^+$

Table 1. **SARS-CoV-2 spike protein variants tested**

		B.1 lineage (D614G)	B.1 + D80Y	B.1 + S98F	B.1 + A222V	B.1 + N439K	B.1 + S477N	B.1 + E484K	B.1 + Y453F, ΔH69, ΔV70	Mink Cluster 5	B.1.1.7 UK (501Y.V1)	B.1.351 + R246I RSA (501Y.V2)	B.1.351 + D215G RSA (501Y.V2)	B.1.351 + D215G + Δ242-244 RSA (501Y.V2)
S1	**NTD**								Δ69–70	Δ69–70	Δ69–70			
1–685	13–305		D80Y									D80A	D80A	D80A
				S98F										
											Δ144			
													D215G	D215G
					A222V									
												L242H	L242H	Δ242–244
												R246I		
	RBD											K417N	K417N	K417N
	330–521					N439K								
									Y453F	Y453F				
							S477N							
								E484K				E484K	E484K	E484K
											N501Y	N501Y	N501Y	N501Y
		D614G	D614G	D614G	D614G	D614G	D614G	D614G	D614G	D614G	D614G	D614G	D614G	D614G
											A570D			
											P681H			
S2										I692V				
686–1273												A701V	A701V	A701V
											T716I			
											S982A			
											D1118H			
										M1229I				

Gray shading indicates the RBD region.

T cells induced by $Al(OH)_3$-adjuvanted spike protein only produced IL-2. None of the immunization regimens induced $CD8^+$ T cells producing significant amounts of IL-4, IL-5, or IL-13 (Fig. S3 B).

Protective efficacy of one- and two-dose Ad26.COV2.S vaccine regimens in aged rhesus macaques

13 wk after the first Ad26.COV2.S dose, the one-dose 10^{11}-vp Ad26.COV2.S group, two-dose 5×10^{10}-vp Ad26.COV2.S group, and the sham control group (Ad26.RSV.gLuc) were inoculated with a total dose of 10^5 tissue culture infective dose 50 ($TCID_{50}$) SARS-COV-2 strain Leiden-0008 by the intranasal and intratracheal routes. To increase statistical power, data from a challenge of naive animals (n = 4) using the identical challenge strain, challenge regimen, and readouts were added to the sham control group data, collectively referred to as pooled control. Viral loads were assessed by RT–quantitative PCR, measuring subgenomic mRNA (sgmRNA; Wölfel et al., 2020) levels in nasal and tracheal swabs daily during the follow-up period. Low levels of virus were detected in the nose and trachea of some vaccinated animals. In the nose, the median number of days that virus was present in each animal was 0.5 d (range, 0–3 d) and in the trachea 2.5 d (range, 1–5 d) for the single-dose 10^{11}-vp Ad26.COV2.S group. For the two-dose 5×10^{10}-vp Ad26.COV2.S group, median number of days virus was present in the nose of each animal was 1 d (range, 0–2 d) and in the trachea 3 d (range, 2–4 d). By contrast, in the pooled control group, virus was present in the nose for the entire follow-up period for all except one animal that was consistently negative for nose viral sgmRNA (median of 7 d; range 0–7 d), while in the trachea the median number of days virus was present was 6 d (range, 4–7 d) for each animal (Fig. S4). Quantification of total viral load in the follow-up period per animal as determined by calculating area under the curve (AUC) showed that total viral load was significantly lower in both vaccinated groups compared with the pooled control group in both samples, from the nose ($P \leq 0.012$; Tobit ANOVA z-test) as well as from the trachea ($P \leq 0.013$; Tobit ANOVA z-test; Fig. 4 A). Bronchoalveolar lavage (BAL) samples were

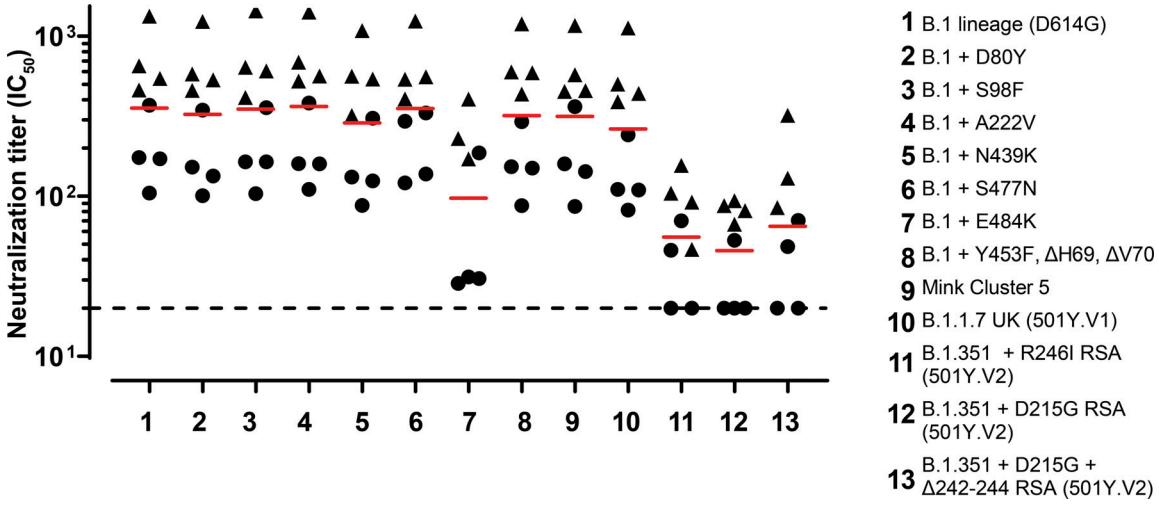

Figure 6. **Neutralizing activity of antibodies elicited by Ad26.COV2.S against SARS-CoV-2– spike variants.** NHPs received 1 × 10^{11} vp Ad26.COV2.S in a one-dose regimen (n = 6) or a two-dose regimen of 5 × 10^{10} vp Ad26.COV2.S (n = 6) or control Ad26.RSV.gLuc (n = 4) at study weeks 0 and 8. Neutralizing antibody titers of a subset (n = 4 per group) of Ad26.COV2.S-immunized NHP serum samples are shown. Dots are week 8 samples from the one-dose 10^{11}-vp treatment group (i.e., 8 wk after the first dose). Triangles are week 10 samples from the two-dose 5 × 10^{10}–vp treatment group (i.e., 2 wk after the second dose). Note that serum from one animal from the two-dose 5 × 10^{10}–vp treatment group was not measured against the B.1 lineage (D614G) + E484K variant and lineage B.1.351 501Y.V2–del242-244 (RSA) due to lack of sufficient volume. Neutralizing antibody titers were below the limit of detection (LOD) in serum from the sham-immunized group, and sera did not have neutralizing antibody titers against the psVNA specificity control (i.e., lentivirus pseudotyped with VSVΔG). Neutralizing antibody titers are expressed as the geometric mean dilution giving a 50% reduction (IC_{50}) in the luciferase readout relative to control wells without any serum added. Individual dots represent individual samples, as a geometric mean of a maximum of four individual assay runs of NHP samples, depending on the variant. Red horizontal bars per SARS-CoV-2–spike variant represent average geometric mean titers of individual NHPs. Dashed horizontal line represents the LOD of a 1:20 dilution. Samples with no measurable titer were set at LOD.

collected at regular intervals during the follow-up period for assessment of viral sgmRNA as well. Only one animal had detectable viral sgmRNA just above the limit of detection in the two-dose Ad26.COV2.S vaccine group, while it was consistently present at high levels in BAL samples from all control animals (Fig. 4 B and Fig. S4). The single-dose Ad26.COV2.S group was not sampled for BAL due to restrictions in the number of animals that can be handled in the Biosafety Level 3 facility. At days 7 and 8, all animals were euthanized and lung tissue was collected. The majority of both one- and two-dose Ad26.COV2.S-vaccinated animals did not show virus above the limit of quantification in any of the lung lobes tested, while all lung lobes from pooled control animals (except one lung lobe from one animal) contained viral sgmRNA, with the majority of these at high levels.

The animals showed no overt clinical signs after virus infection, and clinical chemistry parameters in blood were normal. Body temperature was continuously measured throughout the study. Prechallenge data were used to reconstruct a daily baseline temperature profile for each individual animal. Fever, defined as temperature increase above baseline, was recorded after infection, and total temperature increase during the follow-up period was calculated by means of AUC (fever duration). All animals showed an increase in temperature after SARS-CoV-2 inoculation. A modest yet statistically significant reduction in fever duration was observed for both vaccinated groups compared with the pooled control animal group ($P \leq 0.012$; t test; Fig. 4 D and Fig. S5).

Histological analysis of lung tissue at the end of the study showed minimal pulmonary pathology. The main histological findings were minimal to mild perivascular and peribronchiolar inflammatory infiltrates (cuffing) and minimal to mild mononuclear or mixed cell infiltrates (macrophages and lymphocytes and scattered neutrophils) in alveolar septa and in some alveolar lumina, and focal bronchoalveolar hyperplasia was observed in some vaccinated animals (Fig. 5, A, B, D, and E). SARS-CoV-2 nucleoprotein (N) staining was limited to a few isolated positive pneumocytes in a single lung lobe in 1 out of 11 vaccinated animals (Fig. 5, G and H). By contrast, sham control animals demonstrated evidence of SARS-CoV-2 viral interstitial pneumonia, characterized mostly by thickening of alveolar septa (interstitium) by a moderate mononuclear or mixed cell infiltrate in the interstitium, mild to moderate type II pneumocyte hyperplasia or bronchoalveolar hyperplasia, diffuse alveolar damage, and alveolar lumina containing edema (homogenous eosinophilic fluid) admixed with mononuclear or mixed cell infiltrates, fibrin, and scattered multinucleated syncytial cells (Fig. 5, C and F). Immunohistochemistry staining for SARS-CoV-2 N showed minimal to moderate numbers of SARS-CoV-2 N-positive pneumocytes in multiple lung lobes (Fig. 5 I) in seven out of eight sham control animals, consistent with RT–quantitative PCR data from the lung lobes.

Neutralizing activity of antibodies elicited by Ad26.COV2.S in NHPs against SARS-CoV-2 spike variants

To understand the breadth of neutralization against rapidly spreading SARS-CoV-2 spike variants of concern, we tested serum samples from aged NHPs immunized with one- and two-dose (8-wk interval) Ad26.COV2.S regimens with a lentivirus-based

psVNA against 12 SARS-CoV-2 spike variants harboring single amino acid substitutions and combinations of substitutions as present in currently circulating strains (Table 1). The neutralizing capacity against these spike variants of SARS-CoV-2 was normalized to the neutralizing capacity against the Wuhan spike protein strain with only the D614G substitution (named here B.1 lineage [G614]), representing the dominant circulating strain lineage globally. We selected sera from weeks 8 (one-dose regimen) and 10 (two-dose regimen) after vaccination for testing of neutralizing activity against these new spike variants. Neutralization titers were higher for the two-dose regimen than for the one-dose regimen sera; however, the fold reduction in neutralization for each of the spike protein variants was not statistically significant between the two regimens (*t* test), and results obtained with the one-dose and two-dose regimens were therefore pooled for statistical analysis. Neutralizing antibody titers against spike protein variants with amino acid substitutions in the receptor-binding domain (RBD), including N439K, Y453F, S477N, and N501Y substitutions, and the N-terminal domain (NTD) were relatively similar (i.e., 95% confidence interval within twofold difference, one-sample *t*-test) to those observed against the B.1 lineage (G614; Fig. 6 and Table 1). This also included the lineage B.1.1.7 (UK) and the Mink Cluster 5 variants, which have substitutions in the RBD and deletions in the NTD (amino acids 69–70), as well as additional substitutions in the S1 and/or S2 region (Fig. 6 and Table 1). Neutralizing antibody titers against the variants containing the E484K substitution in the RBD were present but reduced (fold reduction between 3.35–7.78, 95% confidence interval all above twofold difference, one-sample *t* test). The dominant circulating B.1.351 spike variant originating in RSA, which harbors E484K and additional substitutions in the RBD, NTD, and S2 and deletions in the NTD (amino acids 242–244), was neutralized with a 5.02-fold reduced titer (Fig. 6, number 13).

Discussion

We previously reported immunogenicity and protective efficacy data of a single dose of our COVID-19 vaccine candidate Ad26.COV2.S in adult NHPs (Mercado et al., 2020). Here, we evaluated the immunogenicity of one- and two-dose Ad26.COV2.S regimens in adult and aged rhesus macaques for up to 14 wk after the first dose in order to gain insight into the durability of immunity after a single dose of this vaccine candidate and the added value of a second dose on the magnitude of spike protein–specific immune responses. In addition, we assessed the protective efficacy of one- and two-dose Ad26.COV2.S regimens in aged NHPs. We used a new challenge model based on the D614G spike SARS-CoV-2 variant, which emerged in spring 2020 and rapidly became the most prevalent spike variant in most geographies. We also tested the in vitro neutralization breadth of Ad26.COV2-S–elicited antibodies against two of the newly emerging SARS-CoV-2 spike variant lineages, B.1.1.7 and B.1.351, originating from the UK and RSA, respectively (Tegally et al., 2020 *Preprint*; European Centre for Disease Prevention and Control, 2020; World Health Organization, 2020a; Fontanet et al., 2021).

In both adult and aged macaques, spike protein–binding and SARS-CoV-2 neutralizing antibody responses were detected as early as 2 wk after the first Ad26.COV2.S immunization and were significantly increased by week 4 in agreement with our clinical trial observations in adults and elderly after a single immunization with Ad26.COV2.S (Sadoff et al., 2021). In addition, robust neutralization was measured against SARS-CoV-2 isolate Leiden-0008 (spike G614), which is in line with previously reported findings in animal models and humans showing that antibodies elicited by a vaccine or virus bearing the original spike protein D614 were able to neutralize the G614 virus (Plante et al., 2021; Weissman et al., 2021).

Humoral immune responses were maintained at least up to week 14 after immunization, providing an early sign of the durability of immunity elicited by Ad26.COV2.S. Binding and neutralizing antibody responses showed some decline over time, while neutralizing antibody responses appeared to be more stably maintained, especially in recipients of the 5×10^{10}–vp dose level. Although humoral immune responses were initially significantly higher in NHPs that received the 10^{11}-vp dose as compared with recipients of the 5×10^{10}–vp vaccine dose, differences in neutralizing antibody levels decreased over time and do not suggest a clear benefit of the higher dose, in agreement with interim Phase 1/2a clinical data (Sadoff et al., 2021).

A second dose of Ad26.COV2.S given with an 8-wk interval resulted in a significant increase in spike protein–specific binding and neutralizing antibody responses in both adult and aged NHPs. This is in line with our data in humans (Sadoff et al., 2021) and with observations with other Ad26-based vaccines (Geisbert et al., 2011; Callendret et al., 2018; Salisch et al., 2019; Baden et al., 2013; Salisch et al., 2021)

Neutralizing antibody titers were higher in NHPs that received the two vaccine doses 8 wk apart compared with the 4-wk interval, albeit both two-dose regimens were more immunogenic than the one-dose regimen. This confirms that a longer interval between vaccine doses can significantly improve the magnitude and/or quality of the antibody response. (Ledgerwood et al., 2013; Siegrist, 2018; Sallusto et al., 2010; Roozendaal et al., 2020). While we have not evaluated the potential difference in efficacy of longer and shorter two-dose regimens in NHPs, a two-dose regimen of 5×10^{10} vp Ad26.COV2.S administered 8 wk apart is currently being tested for efficacy in humans (ENSEMBLE 2, NCT04614948).

We observed a strong correlation between binding and neutralizing antibody levels in sera from vaccinated adult and aged NHPs across time points. Interestingly, the correlation between binding and neutralizing antibody levels increased over time, with a particularly robust correlation observed from week 6 onward, possibly reflecting antibody affinity maturation and enrichment of neutralizing antibodies over time (Longworth et al., 2002; Victora and Nussenzweig, 2012). The strong correlation between binding and neutralizing antibody levels observed in this study confirms our earlier observation (Yu et al., 2020; Mercado et al., 2020; McMahan et al., 2021) and suggests that spike protein–binding antibody concentrations measured by ELISA could be used as a surrogate readout for neutralizing antibody responses. A full-length spike protein–based ELISA, as

used in the assays reported here, is advantageous compared with an RBD-based ELISA as it would also detect antibodies with neutralizing activity outside the spike RBD domain (Chi et al., 2020).

Almost all Ad26.COV2.S-vaccinated aged NHPs that were challenged 3 mo after first immunization were protected from lung infection, as demonstrated by negative PCR testing for sgmRNA in BAL and lung tissue samples. Detection of SARS-CoV-2 sgmRNA by RT-PCR is a highly sensitive method for the direct measurement of viral replication, which is more sensitive than $TCID_{50}$ or plaque assays (Dagotto et al., 2021). Only one Ad26.COV2.S-vaccinated animal that received a single vaccination had clearly detectable SARS-CoV-2 sgmRNA levels as well as traces of viral antigen detected by immunohistochemistry in lung tissue samples. This animal had much lower binding and neutralizing antibody levels after vaccination, which could explain the breakthrough infection, as in earlier studies protection from infection was correlated with binding and neutralizing antibody titers (Mercado et al., 2020; Yu et al., 2020; McMahan et al., 2021). Nevertheless, viral load in this animal was lower compared with viral load in lungs of challenged control animals. While complete protection apparently requires a higher neutralizing antibody titer in this particular animal model, it is tempting to speculate that the viral load reduction in lung associated with lower neutralizing antibody titers could translate to protection from severe disease even in low human vaccine responders. Indeed, while histological analysis and immunohistochemistry in lung tissue showed severe pulmonary histopathology and presence of viral antigens in challenged control animals, only minimal histopathological abnormalities and viral antigens in lungs of Ad26.COV2.S-vaccinated animals were observed, in agreement with earlier observations (Corbett et al., 2020). We observed a small but persistent decrease in the febrile response after infection in vaccinated animals. Although transient fever has been described after SARS-CoV-2 infection of rhesus macaques (Munster et al., 2020 *Preprint*), no effect on body temperature was observed in recent NHP vaccine efficacy studies (Chen et al., 2020 *Preprint*; Wang et al., 2020). In addition to differences with respect to the NHP models used in other studies, such as age and challenge virus, an important advantage in this study might be that body temperature was continuously monitored and that no additional interventions were required to record body temperature. Continuous temperature monitoring might therefore be a useful clinical parameter in NHP vaccine efficacy models.

The only partial protection of the upper respiratory tract observed in our present study seems at odds with our previous NHP study, in which Ad26.COV2.S elicited immunity providing complete and near-complete protection against viremia in the lung and upper respiratory tract, respectively (Mercado et al., 2020). Several factors may contribute to this difference in outcome. NHPs in our current study were aged, and the time of challenge after immunization was considerably longer, albeit antibody titers were not waning. Additionally, the G614 SARS-CoV-2 challenge strain instead of the Washington D614 challenge strain was used and was reported to be associated with enhanced viral replication in the upper respiratory tract and potentially enhanced viral transmissibility, but with no associated increase in disease severity (Plante et al., 2021; Hou et al., 2020).

Ad26.COV2.S-elicited immunity is protective against SARS-CoV-2 with either the D (Mercado et al., 2020) or the G at amino acid position 614 of the spike protein. However, new SARS-CoV-2 lineages have recently emerged, some of which seem to be more neutralization resistant. Sera from Ad26.COV2.S-immunized NHPs showed similar antibody neutralizing titers against the B.1.1.7 lineage originating from the UK as well as the Mink Cluster 5 compared with titers against the SARS-CoV-2 Wuhan D614G lineage (B.1 lineage [G614]). Furthermore, variants with substitutions in the NTD and S2 region of the spike protein and substitutions in the RBD, including N439K, Y543F, S477N, and N501Y, were neutralized with equal efficiency by the polyclonal NHP sera, although several of these substitutions have been shown to have negative effects on monoclonal antibody binding and neutralization (Thomson et al., 2020 *Preprint*; Planas et al., 2021 *Preprint*). The sera from Ad26.COV2.S-vaccinated NHPs even neutralized B.1.351 SARS-CoV-2 lineage variants that first emerged in RSA and harbors the E484K and other substitutions in the RBD, albeit with five- to eightfold reduced titers, in line with observations with other vaccine-elicited immune sera (Xie et al., 2021; Wu et al., 2021 *Preprint*).

Another important aspect in the development of COVID-19 vaccines is de-risking for the potential and theoretical risk of Vaccine-Associated Enhanced Respiratory Disease (Lee et al., 2020; Bottazzi et al., 2020; Haynes et al., 2020), which is generally considered to be associated with nonneutralizing antibody responses and Th2-skewed cellular immunity. Here, we show that in aged NHPs, Ad26.COV2.S elicited $CD4^+$ T cell responses that were Th1 skewed, confirming our observations in elderly humans (Sadoff et al., 2021) and similar to findings with other genetic vaccine platforms encoding the SARS-CoV-2 spike protein (van Doremalen et al., 2020; Yu et al., 2020; Anderson et al., 2020; Vogel et al., 2020 *Preprint*; Corbett et al., 2020). The ability of NHPs to develop a Th2 cell–skewed immune response was demonstrated by vaccination with an $Al(OH)_3$-adjuvanted spike protein. The Th1 cell–skewed response in Ad26.COV2.S-vaccinated NHPs together with the induction of robust and durable neutralizing antibody responses by Ad26.COV2.S and the absence of enhanced lung pathology in challenged animals indicate that the potential for Vaccine-Associated Enhanced Respiratory Disease with this vaccine is extremely unlikely.

Overall, the immunogenicity, protective efficacy, and SARS-CoV-2 spike variant neutralizing data presented in this manuscript further support our decision to evaluate a single 5×10^{10}–vp dose of Ad26.COV2.S in our Phase 3 ENSEMBLE (Trial Number: NCT04505722) study and also to evaluate a two-dose Ad26.COV2.S regimen in our second Phase 3 study ENSEMBLE 2 (Trial Number: NCT04614948).

Materials and methods

Animals

Adult NHPs

The NHP study of adult animals was conducted at Charles River Laboratories Montreal ULC, Laval Site (CA). Animals were

obtained from Kunmings Biomed International Ltd, China. Prior to transfer from the test facility colony, all animals were subjected to a health assessment and were tested at least once for tuberculosis by intradermal injection of tuberculin. An anthelmintic treatment was administered to each animal by subcutaneous injection. The evaluations were performed in accordance with standard operating procedures by technical staff. Animal experiment approval was provided by the Institutional Animal Care and Use Committee at Charles River Laboratories Montreal ULC, Laval Site (CA). Animal experiments were performed in compliance with guidelines published by the Canadian Council on Animal Care and the Guide for the Care and Use of Laboratory Animals published by the National Research Council Canada. The Test Facility is accredited by the Canadian Council on Animal Care and the American Association for Accreditation of Laboratory Animal Care. In addition, the study was conducted according to European Medicines Agency guideline International Conference on Harmonisation M3(R2): Guidance on Non-Clinical Safety Studies for the Conduct of Human Clinical Trials and Marketing Authorization for Pharmaceuticals and Food and Drug Administration guideline, Redbook 2000: General Guidelines for Designing and Conducting Toxicity Studies.

Aged NHPs

The study using aged NHPs was performed at the Biomedical Primate Research Centre, Rijswijk, Netherlands (an American Association for Accreditation of Laboratory Animal Care–accredited institution). Animals were captive-bred for research purposes and socially housed. Animal housing was according to international guidelines for NHP care and use (The European Council Directive 2010/63, and Convention ETS 123, including the revised Appendix A as well the "Standard for humane care and use of Laboratory Animals by Foreign institutions" identification number A5539-01, provided by the Department of Health and Human Services of the US National Institutes of Health). The study was conducted in compliance with and approved by all relevant local and national regulations, and the Institutional Animal Welfare Body (Instantie voor Dierenwelzijn, IvD) controlled that all possible precautions were taken to ensure the welfare of and to avoid any unnecessary discomfort to the animals.

Vaccines

The Ad26.COV2.S vaccine was generated as previously described (Bos et al., 2020). Briefly, Ad26.COV2.S is a replication-incompetent Ad26 vector encoding a prefusion-stabilized SARS-COV-2 spike protein sequence (Wuhan-Hu-1; GenBank accession no. MN908947). Replication-incompetent, E1/E3–deleted Ad26-vectors were engineered using the AdVac system (Abbink et al., 2007), using a single plasmid technology containing the Ad26 vector genome including a transgene expression cassette. The human codon–optimized, prefusion-stabilized SARS-COV-2 spike protein–encoding gene was inserted into the E1 position of the Ad26 vector genome. Manufacturing of the Ad26 vector was performed in the complementing cell line PER.C6 TetR (Wunderlich et al., 2018; Zahn et al., 2012). The negative control vector Ad26.RSV.gLuc encodes the RSV F protein fused to *Gaussia* firefly luciferase as a single transgene separated by a 2A peptide sequence, resulting in expression of both individual proteins. Manufacturing of the vector was performed in PER.C6 (Sanders et al., 2013).

The full-length spike protein used for immunization (COR200099; Bos et al., 2020) was produced on Expi293F cells. COR200099 is based on the Wuhan-Hu-1 SARS-CoV-2 strain (GenBank accession no. MN908947) and stabilized by two point mutations (R682A, R685G) in the S1/S2 junction that disrupts the furin cleavage site and by two consecutive prolines (K986P, V987P) in the hinge region in S2. In addition, the transmembrane and cytoplasmic regions have been replaced by a fibritin foldon domain for trimerization and a C-tag, allowing the protein to be produced and purified as soluble protein. Adenoviral vectors and protein were tested for bioburden and endotoxin levels before use.

Study design animal experiments

Adult NHPs

60 (57 females and 3 males; 3 males were allocated to test groups 3, 4, and 5, 1 male in each group) rhesus macaques (*M. mulatta)* from Chinese origin, between 3.3 and 5.0 yr of age and weighing between 2.9 and 8.1 kg, were assigned to five groups by a randomizing stratification system based on body weights. 14 animals were included in each vaccine group, and four animals were included in the sham control group. Group 1 (n = 4) is the sham control group and received saline injection at week 0 and week 8. Groups 2 and 3 (n = 14 in each group) received one immunization with 10^{11} vp and 5×10^{10} vp of Ad26.COV2.S, respectively, at week 0. Groups 4 and 5 (n = 14 in each group) received two immunizations with 5×10^{10} vp of Ad26. COV.2 spaced by 4 (week 0 and week 4) and 8 wk (week 0 and week 8), respectively. All immunizations were performed via the intramuscular route in the quadriceps muscle of the left hind leg. Blood for serum was obtained before the first vaccine dose and every 2 wk subsequently up to week 14 of the study.

Aged NHPs

20 female rhesus macaques (*M. mulatta)* from Indian origin, between 13.8 and 21.9 yr of age and weighing between 6.6 and 12.6 kg, were distributed over four experimental treatment groups and housed in ABSL-III facilities, pair-housed with socially compatible animals. Prior to study start, an AnipillV2 telemetry system (BodyCAP) was surgically implanted in the abdomen of animals and recorded body temperature every 15 min. Group 1 (n = 6) received 10^{11} vp of Ad26.COV2.S at week 0. Group 2 (n = 6) received 5×10^{10} vp of Ad26.COV2.S at weeks 0 and 8. Group 3 (n = 4) received 100 µg spike protein, adjuvanted with 500 µg $Al(OH)_3$ (2% Alhydrogel; InvivoGen) at weeks 0 and 8. The sham control group (Group 4, n = 4) was immunized with 10^{11} vp Ad26.RSV.gLuc, an Ad26 vector expressing an irrelevant antigen, especially to exclude a protective effect by the Ad26 vector against SARS-CoV-2 challenge that would not be related to adaptive spike-specific immunity. All immunizations were performed intramuscularly in the quadriceps of the left hind leg. Blood for serum and PBMC isolation was obtained as indicated in the text.

5 wk after the second vaccination dose, all groups except the $Al(OH)_3$-adjuvanted spike protein group were inoculated with 10^5 $TCID_{50}$ of SARS-CoV-2 isolate Leiden-0008. Clinical isolate SARS-CoV-2/human/NLD/Leiden-0008/2020 (Leiden-0008) was isolated from a PCR-positive throat swab and passaged twice in Vero E6 cells. The spike protein of this isolate contains the D614G mutation. The NGS-derived complete genome sequence of this virus isolate is available under GenBank accession no. MT705206.1 and showed only minor variants from the consensus sequence, especially in the spike furin cleavage site region, where we detected below 2% of heterogeneity. Isolate Leiden-0008 was propagated and titrated in Vero E6 cells. The inoculum was administered in a 2-ml volume, 1 ml intratracheally, just below the vocal cords, and 1 ml intranasally, 0.5 ml per nostril. After virus inoculation, nose and trachea swabs were taken daily, as well as BAL every other day from the two-dose 5×10^{10}–vp Ad26.COV2.S and sham control groups to measure viral load. As animals were anesthetized on a daily basis, tube feeding was applied. Animals were euthanized at days 7 and 8 after virus inoculation, with the number of animals of each group evenly distributed over both days, and respiratory tract tissues were isolated for histopathology, immunohistochemistry, and viral load. To increase statistical power, the data from the sham control group was pooled with data from the pilot virus inoculation study, consisting of naive animals ($n = 4$) of the same age range that were inoculated identically as described above for the vaccine study. One animal in the 5×10^{10}–vp Ad26.COV2.S group died during the study. Postmortem autopsy identified a marked to severe, acute bronchopneumonia associated with foreign particulate material in the airways, which is consistent with aspiration pneumonia in the lung as the cause of death of this animal. The death was therefore deemed unrelated to the vaccine, and the animal was excluded from all other analyses.

ELISA

IgG binding to SARS-CoV-2 spike protein was measured by ELISA using a recombinant spike protein antigen based on the Wuhan-Hu-1 SARS-CoV-2 strain (GenBank accession no. MN908947). The SARS-CoV-2 spike protein antigen was adsorbed on 96-well microplates for a minimum of 16 h at 4°C. Following incubation, plates were washed in PBS/0.05% Tween-20 and blocked with 5% skim milk in PBS/0.05% Tween-20 for 1 h at room temperature. Serum standards, controls, and NHP serum samples were diluted and incubated on the plates for 1 h at room temperature. Next, the plates were washed and incubated with peroxidase-conjugated goat anti-human IgG for 1 h at room temperature, washed, and developed with tetramethylbenzidine substrate for 30 min at room temperature and protected from light, then stopped with H_2SO_4. The optical density was read at 450/620 nm. The antibody concentrations were back calculated on the standard, and the reportable values were generated based on all passing dilutions, expressed in ELISA units (EU)/ml. The lower limit of detection (LLOD) is 3.4 EU/ml, based on the standard lowest interpolation range concentration multiplied per the dilution factor and is used as an informative LLOD. LLOQ is based on qualification performed for human samples and has been set at 50.3 EU/ml.

psVNA

For assessing the immunogenicity elicited by Ad26.COV2.S, SARS-CoV-2 spike-neutralizing antibody titers were measured by psVNA. Pseudotyped virus particles were made from a modified Vesicular Stomatitis Virus (VSVΔG) backbone and bear the spike glycoprotein of the Wuhan SARS-CoV-2 strain (based on Wuhan-Hu-1; GenBank: accession no. MN908947). The pseudoparticles contain a luciferase reporter gene used for detection. Serial dilutions of heat-inactivated NHP serum samples were prepared in 96-well transfer plates. The SARS-CoV-2 pseudovirus was added sequentially to the serum dilutions and incubated at 37°C with 5% CO_2 supplementation for 60 ± 5 min. Serum–virus complexes were then transferred onto plates previously seeded overnight with Vero E6 cells and incubated at 37°C and 5% CO_2 for 20 ± 2 h. Following this incubation, the luciferase substrate was added to the cells in order to assess the level of luminescence per well. The plates were then read on a luminescence plate reader. The intensity of the luminescence was quantified in relative luminescence units (RLUs). The neutralizing titer of a serum sample was calculated as the reciprocal serum dilution corresponding to the 50% neutralization antibody titer (inhibitory concentration $[IC]_{50}$) for that sample. The LLOD is 10, which is the first sample dilution (1:10) used as an informative LLOD. LLOQ is based on qualification performed for human samples and has been set on 33 IC_{50}.

For measuring the breadth of neutralization against SARS-CoV-2 spike variants, SARS-CoV-2 spike-neutralizing antibody titers were measured by psVNA against several SARS-CoV-2 spike variants. For the generation of pseudotyped HIV-based lentiviruses, the DNA coding for SARS-COV-2 Spike protein (based on Wuhan-Hu-1; GenBank accession no. MN908947) C-terminally truncated by 19 amino acids was cloned into a derivative of the pCDNA3.1 expression vector (Thermo Fisher Scientific) containing a CMV promoter and a Bovine Growth Hormone polyadenylation signal. Gene sequences were codon optimized and synthesized. Substitutions and deletions in the Spike protein gene open reading frame were introduced using standard molecular biology techniques and confirmed by sequencing. All the SARS-CoV-2 Spike protein variants generated are summarized in Table 1. HIV-based lentiviral pseudotyped particles harboring the SARS-CoV-2 Spike protein variants were produced using the ViraPower Lentiviral Expression system (Thermo Fisher Scientific) according to manufacturer's protocol with some minor changes. In short, pseudoviruses expressing a luciferase reporter gene were generated by transfecting Hek293FT cells with a mixture of plasmids (pLP1, pLP2, and pLenti6/Luc) supplying the structural and replication proteins required to produce lentivirus and the plasmid encoding the SARS-CoV-2 S variant. The plasmids were transfected in a ratio of 33:33:33:1, respectively, using Lipofectamine 2000 Transfection Reagent according to manufacturer's protocol (Thermo Fisher Scientific). Cells were incubated overnight at 37°C, 10% CO_2 in Opti-MEM supplemented with 5% FBS. The next day, medium was replaced with Opti-MEM supplemented with 5%

FBS and 1% PenStrep. After 48 h, vp productions were harvested and centrifuged at 300 ×*g* for 5 min. Supernatant containing the pseudotyped lentiviral particles was aliquoted and stored in single-use cryovials at −80°C. To determine the neutralizing activity of NHP sera, assays were performed on Hek293T target cells stably expressing the human ACE2 and human *TMPRSS2* genes (VectorBuilder; Cat. CL0015; Neerukonda et al., 2020 *Preprint*). The cells were seeded in white half-area 96-well tissue culture plates (Perkin Elmer) at a density of 1.5 × 10^4 cells/well (50 µl) and incubated overnight. Heat-inactivated (60 min at 56°C) serum samples were twofold serial diluted over 10 columns in phenol red free DMEM supplemented with 1% FBS and 1% PenStrep. The serial diluted serum samples were incubated at room temperature with an equal volume of pseudovirus particles with titers of ∼1 × 10^5 RLUs luciferase activity. After 1-h incubation, 50 µl of the serum-particle mixture was inoculated onto Hek293T.ACE2.TMPRSS2 cells. Luciferase activity was measured 40 h after transduction by adding an equal volume of NeoLite substrate (Perkin Elmer) to the wells according to the manufacturer's protocol, followed by readout of RLUs on the EnSight Multimode Plate Reader (Perkin Elmer). SARS-CoV-2 neutralizing titers were calculated as the sample dilution at which a 50% reduction (IC_{50}) of luciferase readout was observed compared with luciferase readout in the absence of serum ("High Control").

Wild-type virus neutralization assay (VNA)

Leiden University Medical Center (LUMC) neutralization assays against live SARS-CoV-2 were performed using the microneutralization assay as previously described (Bos et al., 2020), with the modification of a different strain used, SARS-CoV-2 isolate Leiden-0008. The Leiden-0008 virus (GenBank accession no. MT705206.1) was propagated and titrated in Vero E6 cells using the $TCID_{50}$ endpoint dilution method, and the $TCID_{50}$ was calculated by the Spearman-Kärber algorithm as previously described (Hierholzer and Killington, 1996). All work with live SARS-CoV-2 was performed in a Biosafety Level 3 facility at LUMC. Vero-E6 cells were seeded at 12,000 cells/well in 96-well tissue culture plates 1 d before infection. Heat-inactivated (30 min at 56°C) serum samples were analyzed in duplicate. The panel of sera was twofold serially diluted in duplicate, with an initial dilution of 1:10 and a final dilution of 1:1,280 in 60 µl Eagle's MEM supplemented with penicillin, streptomycin, 2 mM L-glutamine, and 2% FCS. Diluted sera were mixed with equal volumes of 120 $TCID_{50}$/60 µl Leiden-0008 virus and incubated for 1 h at 37°C. The virus-serum mixtures were then added onto Vero E6 cell monolayers and incubated at 37°C in a humidified atmosphere with 5% CO_2. Cells either unexposed to the virus or mixed with 120 $TCID_{50}$/60 µl SARS-CoV-2 were used as negative (uninfected) and positive (infected) controls, respectively. At 3 d after infection, cells were fixed and inactivated with 40 µl 37% formaldehyde/PBS solution/well overnight at 4°C. The fixative was removed from cells, and the clusters were stained with 50 µl/well crystal violet solution, incubated for 10 min, and rinsed with water. Dried plates were evaluated for viral cytopathic effect. Neutralization titer was calculated by dividing the number of positive wells with complete inhibition of the virus-induced cytopathogenic effect by the number of replicates and adding 2.5 to stabilize the calculated ratio. The neutralizing antibody titer was defined as the $\log_2$ reciprocal of this value. A SARS-CoV-2 back-titration was included with each assay run to confirm that the dose of the used inoculum was within the acceptable range of 30–300 $TCID_{50}$.

Neutralizing antibodies capable of inhibiting wild-type virus infections were quantified using also the wild-type virus microneutralization assay that was developed and qualified for human samples by Public Health England (PHE). The virus stocks used were derived from the Victoria/1/2020 strain (GenBank accession no. MT007544.1). In brief, six twofold serial dilutions of the heat-inactivated NHP serum samples were prepared in 96-well transfer plate(s). The SARS-CoV-2 wild-type virus was subsequently added to the serum dilutions at a target working concentration (∼100 PFU/well) and incubated at 37°C for 60–90 min. The serum-virus mixture was then transferred onto assay plates previously seeded overnight with Vero E6 cells and incubated at 37°C and 5% CO_2 for 60–90 min before the addition of carboxymethyl cellulose overlay medium and further incubation for 24 h. Following this incubation, the cells were fixed and stained using an antibody pair specific for the SARS-CoV-2 RBD of the spike protein, and immunoplaques were visualized using TrueBlue substrate. Immunoplaques were counted using an Immunospot Analyzer (Cellular Technology Limited). The immunoplaque counts were exported to SoftMax Pro (Molecular Devices), and the neutralizing titer of a serum sample was calculated as the reciprocal serum dilution corresponding to the 50% neutralization antibody titer (IC_{50}) for that sample.

Ad26 neutralization assay

Ad26 neutralizing antibody titers in serum were assessed using a luciferase-based VNA. Briefly, an E1/E3–deleted Ad26-luciferase reporter construct was added to 96-well half-area tissue culture–treated plates (Greiner) at a multiplicity of infection of 1,000, together with twofold serial dilutions of individual heat-inactivated serum samples starting at a 1:16 dilution in a total volume of 25 µl. After 1 h, A549 human lung carcinoma cells (catalog number ATCC CCL-185, obtained from the American Type Culture Collection) were added at a density of 1 × 10^4 cells/well. After incubation for 20 h at 37°C and 10% CO_2, luciferase activity was measured using the Neo-Lite Luciferase Assay System (Perkin Elmer), and an EnVision multimode plate reader (Perkin Elmer). 90% neutralization titers (IC_{90}) were defined as the maximum serum dilution that neutralized 90% of luciferase activity. Each serum sample was analyzed in duplicate.

ELISPOT

IFN-γ/IL-4 Double-Color was performed on freshly isolated PBMCs. PBMCs were isolated from EDTA whole blood using Ficoll gradient centrifugation (10 ml 92% Ficoll-Paque Plus [GE Healthcare] in 1:4 Dulbecco's PBS diluted blood). The ELISPOT was performed using the ImmunoSpot Human IFN-γ/IL-4 Double-Color Enzymatic ELISPOT Assay Kit according to the manufacturer's protocol (Cellular Technology Limited).

Ethanol-activated 96-well ELISPOT plates were coated overnight with anti-human IFN-γ and IL-4 capture antibodies. Cells were plated at a concentration of 250,000 cells per well and stimulated with either cell culture medium in the presence of DMSO, two pools of consecutive 15-mer peptides with 11 amino acid overlap (JPT) spanning the entire length of the SARS-CoV-2 spike protein at a peptide concentration of 2 µg/ml, or 1 µg/ml PHA as positive control for 22 h. Analysis was performed using the ImmunoSpot Analyzer and ImmunoSpot Software (Cellular Technology). Spot-forming units per 1×10^6 PBMCs were calculated by subtraction of medium stimulus counts of the individual peptide pools per animal and summed across the two peptide pools.

ICS

For analysis of intracellular cytokine expression, 10^6 freshly isolated PBMCs were stimulated at 37°C overnight (~15 h) with either cell culture medium in the presence of DMSO and 2 µg/ml SARS-CoV-2 spike protein peptide pools (as described for ELISPOT) or 5 µg/ml PHA in the presence of GolgiStop (BD Biosciences). Stimulated cells were first incubated with LIVE/DEAD Aqua viability dye (Thermo Fisher Scientific), followed by surface staining with anti-human monoclonal antibodies CD3-PerCP-Cy5.5 (clone SP34-2, cat. no. 552852), CD4-APC H7 (clone L200, cat. no. 560837), CD8-BV650 (clone SK1, cat. no. 565289), CD14-BV605 (clone M5E2, cat. no. 564054), and CD69-BV786 (clone FN50, cat. no. 563834), all from BD Biosciences, and CD20-BV605 (BioLegend; clone 2H7, cat. no. 302334). Cells were subsequently fixed with Cytofix/Cytoperm buffer (BD Biosciences) and stained intracellularly with anti-human IL-2–PE (clone MQ1-17H12, cat. no. 560709), IFN-γ–APC (clone B27, cat. no. 554702) from BD Biosciences; IL-5-Vio515 (clone JES1-39D10, cat. no. 130–108-099; Miltenyi Biotec); and IL-4–PE Dazzle594 (clone MP4-25D2, cat. no. 500832) and IL-13–BV421 (clone JES10-5A2, cat. no. 501916), both from BioLegend. Sample acquisition was performed on an LSR Fortessa (BD Biosciences), and data were analyzed in FlowJo V10 (TreeStar). Antigen-specific T cells were identified by consecutive gating on single cells (forward scatter [FSC]-H versus FSC-A), live cells, size (lymphocytes; FSC-A versus side scatter-A), $CD3^+$, $CD4^+$, or $CD8^+$ cells, and $CD69^+$ plus cytokine-positive. Cytokine-positive responses are presented after subtraction of the background response detected in the corresponding medium-stimulated sample of each individual animal. Responders were defined by a technical threshold (Bowyer et al., 2018), the theoretical ability to detect at least one event in a cytokine gate, and are here defined as the reciprocal of the average number of $CD4^+$ or $CD8^+$ T cells of the medium- and peptide pool–stimulated samples for each assay run. $CD4^+$ Th1 cell and Th2 cell subsets were defined by Boolean gating. The Th1 cell subset consists of $CD4^+CD69^+$ T cells expressing IFN-γ and/or IL-2 but not IL-4, IL-5, and IL-13. The Th2 cell subset was defined as $CD4^+CD69^+$ T cells expressing IL-4 and/or IL-5 and/or IL-13.

RNA isolation and SARS-CoV-2 sgmRNA assay

RNA was extracted from homogenized lung tissue and from BAL fluid, trachea, and nasal swabs by use of the QIAamp Viral RNA Mini Kit (Qiagen) according to manufacturer's instructions. Viral E gene–derived sgmRNA was quantified using the SuperScript III One-Step RT-PCR System with Platinum Taq DNA Polymerase (Invitrogen), with 400-nM concentration of the forward or reverse primer and 200 nM of probe in a 25-µl reaction. The sequence of the subgenomic leader–specific forward primer as well as the E-gene–specific reverse primer and probe were previously published (Wölfel et al., 2020). RT was performed at 50°C for 15 min, followed by enzyme activation at 95°C for 2 min and 40 PCR cycles of 95°C for 15 s and 60°C for 30 s. An RNA standard was prepared from a pcDNA3.1 plasmid containing the complete E gene behind the SARS-CoV-2 subgenomic leader sequence (nucleotides 1–77 of the SARS-CoV-2 genome). Serial dilution of sgmRNA standard with known number of copies was taken along to calculate sgmRNA in copies per milliliter for swabs or copies per gram tissue. The LLOQs were 2.1×10^3 copies per milliliter and 1×10^4 copies per gram tissue, except for the naive animals that contributed to the pooled control group, for which the LLOQs were 1.1×10^4 copies per milliliter and 5×10^4 copies per gram tissue.

Body temperature analysis

A baseline 24-h body temperature cycle was reconstructed per animal using a multiday window before virus inoculation in which no biotechnical interventions occurred. Fever duration, defined as the net increase in body temperature, was calculated as difference relative to the mean of the baseline cycle at corresponding clock times during the first 6 d of the follow-up period. The lower limit of the temperature difference with the baseline was set at zero to reduce the impact of lower body temperatures during daily postchallenge anesthesia, and the AUC of the net temperature increase in this period was calculated.

Lung gross pathology, histopathology, and immunohistochemistry

At the end of the follow-up period, all animals were necropsied by opening the thoracic and abdominal cavities, and all major organs were examined. The extent of pulmonary consolidation was assessed based on visual estimation of the percentage of affected lung tissue. Nasal mucosa, pharynx, trachea, bronchi, and all lung lobes were collected for histopathological examination and analysis by immunohistochemistry. All tissues were immersed in 10% neutral-buffered formalin for fixation, paraffin embedded, and stained with H&E for histopathological evaluation. The H&E stained tissue sections were examined by light microscopy (Zeiss Axioplan). For immunohistochemistry, paraffin sections of all lung lobes were automatically stained (Ventana Discovery Ultra; Roche) using rabbit polyclonal anti–SARS-CoV Nucleocapsid protein antibody (Novus; NB100-56576). The immunohistochemically stained tissue sections were examined by light microscopy using a Leica DM2500 light microscope with magnification steps of 25×, 50×, 100×, 200×, and 400×.

Statistical analysis

ELISA and psVNA

For Nexelis ELISA binding and psVNA neutralizing antibody data, comparisons between specific vaccine groups were made

with the two-sample *t* test in an ANOVA. Successive time points were compared using the paired *t* test per vaccine group. P values were calculated on log_{10}-transformed values. For lentiviral-based psVNAs, the fold-reduction in psVNA titer of mutant variants relative to the wild-type B.1 D614G variant per subject was calculated from the geometric mean titers across assay replicates per subject. A one-sample *t* test was applied to the log-transformed fold-reduction for each mutant variant per species.

Wild-type VNA

Vaccine groups were compared with the negative control group with the Mann-Whitney *U* test. To account for censoring with titers at LLOD, pairwise comparison between vaccine groups was performed using Tobit ANOVA with vaccine as factor if <50% of the titers were at LLOD. The pairwise comparisons between vaccines were done with the z-test. If, for an assay, any vaccine group had 50% censoring or more, then the pairwise comparisons were done with the Mann-Whitney *U* test.

The difference in titer between consecutive time points was calculated per animal for each assay.

Depending on the number of censored measurements, the differences were compared with a Tobit ANOVA followed by a post hoc z-test or a sign test.

For all statistical tests, the significance level was 5%. No multiple comparison adjustment was applied. All statistical calculations were done in SAS 9.4 (SAS Institute Inc).

Correlation analysis

Correlation coefficients between binding antibody concentrations and neutralizing antibody titers or different neutralization assays were calculated using two-sided Spearman rank correlation.

Challenge data

Mean nasal and trachea swab AUC values of each group were pairwise compared using Tobit ANOVA with post hoc z-test. Mean net temperature difference AUCs were pairwise compared between groups by *t* test.

Online supplementary material

Fig. S1 shows Ad26 neutralizing antibodies at indicated time points. Fig. S2 shows correlation between SARS-CoV-2 neutralizing antibody titers as measured by different VNA assays. Fig. S3 shows Spike protein–specific CD4 and CD8 T cell responses as measured by ICS at the indicated time points. Fig. S4 shows viral load (sgmRNA copies/ml) kinetics in swabs and BAL after SARS-CoV-2 inoculation of vaccinated aged rhesus macaques. Fig. S5 shows body temperatures after SARS-CoV-2 inoculation of vaccinated aged rhesus macaques on day of infection and for 6 consecutive d afterward.

Acknowledgments

We thank the team of Charles River Laboratories Montreal ULC, Laval Site (CR-LAV; Canada), and Reno, NV, Site (US) for their accurate and punctual work on the NHP study with adult macaques; in particular, we thank Anne Marie Downey, Roula Salame, Carolyne Dumont, Rajen Patel, and Sunjay Sethi. We thank the Nexelis Team of the Laval site, Canada, for their speed and flexibility in accommodating spike protein ELISA and psVNA sample analysis within short time lines; in particular, we thank Luc Gagnon, Helen Diamantakis, Mary Osei-Twum, Greg Kulnis, Steven-Phay Tran, Julien St-Jean, Marcel Dupelle, and Akeel Baig. We thank the Microneutralization Assay Testing Team, PHE, Porton Down, Salisbury, UK, for the immunogenicity testing; in particular, we thank Dr. Sue Charlton, Dr. Lorna McInroy, Anna England, Durga Rajapaksa, Stephanie Leung, Lauren Allen, Emily Brunt, Dr. Kevin Bewley, Dr. Naomi Coombes, Imam Shaik, and Dr. Holly Humphries. From LUMC, we thank Ali Tas for his assistance with preparing the SARS-CoV-2/Leiden-0008 challenge virus used in this study and Shessy Torres for excellent technical support. We thank Johan Verspuij for assistance with data processing, Sarah Janssen for ad hoc statistical support, and Janssen colleagues of the Vector Generations and Sub-Unit Vaccine Design departments for providing reagents. We thank Theo Schouten, Taco Uil, and Ronald Vogels for generating the SARS-CoV-2 variants pseudoparticle used in neutralizing assays; Daphne Bouwens, Ilona Bisschop, Jorn Staal, Sonja Schmit-Tillemans, and Johan Verspuij for psVNA execution, and Yolinda van Polanen for help with the Ad26-neutralizing antibody assay. We are grateful to colleagues of the Non-Clinical Safety Toxicology/Pathology Department of Janssen Research and Development in Beerse, Belgium, for performing sectioning, histology staining, and analysis. We thank Gert Scheper, Danielle van Manen, Martin Friedrich Ryser, and Joanne Wolter for reviewing the paper and for providing valuable input. We thank Daniella Mortier, Gwendoline Kiemenyi-Kayere, Zahra Fagrouch, Nikki van Driel, Ivonne Nieuwenhuis, Herman Oostermeijer, Lisette Meijer, Henk Niphuis, Ed Remarque, Tom G.M. Haaksma, and Boudewijn Ouwerling from the Biomedical Primate Research Centre for logistical and biotechnical support.

This project was funded in part by the US Department of Health and Human Services Biomedical Advanced Research and Development Authority under contract HHS0100201700018C.

Author contributions: Designed studies and reviewed data: L. Solforosi, H. Kuipers, M. Jongeneelen, S.K. Rosendahl Huber, J.E.M. van der Lubbe, L. Dekking, R. Roozendaal, B. Brandenburg, H. Schuitemaker, F. Wegmann, and R.C. Zahn. Performed experiments and analyzed data: M. Jongeneelen, D.N. Czapska-Casey, A. Izquierdo Gil, M.R.M. Baert, J. Drijver, J. Vaneman, E. van Huizen, Y. Choi, J. Vreugdenhil, S. Kroos, A.H. de Wilde, E. Kourkouta, R. van der Vlugt., D. Veldman, J. Huizingh, K. Kaszas, T.J. Dalebout, S.K. Myeni, M. Kikkert, E.J. Snijder, K.P. Böszörményi, M.A. Stammes, I. Kondova, E.J. Verschoor, B.E. Verstrepen, G. Koopman, P. Mooij, W.M.J.M. Bogers, M. van Heerden, L. Muchene, J.T.B.M. Tolboom. Contributed to the conception of the work: J. Custers, D.H. Barouch, F. Wegmann, and R.C. Zahn. Drafted the paper: L. Solforosi, H. Kuipers. Reviewed the paper: all authors.

Disclosures: M.R.M. Baert, Y. Choi, J. Custers, D.N. Czapska-Casey, A.H. de Wilde, J. Drijver, J. Huizingh, M. Jongeneelen, K.

Kaszas, E. Kourkouta, H. Kuipers, L. Muchene, R. Roozendaal, S.K. Rosendahl Huber, L. Solforosi, J.T.B.M. Tolboom, J.E.M. van der Lubbe, R. van der Vlugt, M. van Heerden, E. van Huizen, J. Vaneman, D. Veldman, J. Vreugdenhil, and R. Zahn are employees of Janssen Pharmaceutical Companies of Johnson & Johnson. D.H. Barouch reports grants from Janssen during the conduct of the study; grants from NIH, HJF/WRAIR, BMGF, DARPA, Gilead, Intima, Alkermes, CureVac, South Africa MRC, amfAR, Ragon Institute, MassCPR, Sanofi, Legend, and Zentalis; and personal fees from SQZ Biotech outside the submitted work. In addition, D.H. Barouch has a patent to COVID-19 vaccines licensed (Janssen). H. Schuitemaker reports "other" from Department of Health and Human Services BARDA (HHS0100201700018C) during the conduct of the study; and personal fees from Johnson & Johnson and Janssen Vaccines & Prevention B.V. outside the submitted work. F. Wegmann reports a patent to company pending and is an employee of Janssen Pharmaceutical Companies of Johnson & Johnson. No other disclosures were reported.

Submitted: 31 December 2020
Revised: 25 February 2021
Accepted: 8 April 2021

References

Abbink, P., A.A.C. Lemckert, B.A. Ewald, D.M. Lynch, M. Denholtz, S. Smits, L. Holterman, I. Damen, R. Vogels, A.R. Thorner, et al. 2007. Comparative seroprevalence and immunogenicity of six rare serotype recombinant adenovirus vaccine vectors from subgroups B and D. *J. Virol.* 81: 4654–4663. https://doi.org/10.1128/JVI.02696-06

Anderson, E.J., N.G. Rouphael, A.T. Widge, L.A. Jackson, P.C. Roberts, M. Makhene, J.D. Chappell, M.R. Denison, L.J. Stevens, A.J. Pruijssers, et al. mRNA-1273 Study Group. 2020. Safety and Immunogenicity of SARS-CoV-2 mRNA-1273 Vaccine in Older Adults. *N. Engl. J. Med.* 383: 2427–2438. https://doi.org/10.1056/NEJMoa2028436

Baden, L.R., S.R. Walsh, M.S. Seaman, R.P. Tucker, K.H. Krause, A. Patel, J.A. Johnson, J. Kleinjan, K.E. Yanosick, J. Perry, et al. 2013. First-in-human evaluation of the safety and immunogenicity of a recombinant adenovirus serotype 26 HIV-1 Env vaccine (IPCAVD 001). *J. Infect. Dis.* 207: 240–247. https://doi.org/10.1093/infdis/jis670

Baden, L.R., H.M. El Sahly, B. Essink, K. Kotloff, S. Frey, R. Novak, D. Diemert, S.A. Spector, N. Rouphael, C.B. Creech, et al. COVE Study Group. 2021. Efficacy and Safety of the mRNA-1273 SARS-CoV-2 Vaccine. *N. Engl. J. Med.* 384:403–416. https://doi.org/10.1056/NEJMoa2035389

Bos, R., L. Rutten, J.E.M. van der Lubbe, M.J.G. Bakkers, G. Hardenberg, F. Wegmann, D. Zuijdgeest, A.H. de Wilde, A. Koornneef, A. Verwilligen, et al. 2020. Ad26 vector-based COVID-19 vaccine encoding a prefusion-stabilized SARS-CoV-2 Spike immunogen induces potent humoral and cellular immune responses. *NPJ Vaccines.* 5:91. https://doi.org/10.1038/s41541-020-00243-x

Bottazzi, M.E., U. Strych, P.J. Hotez, and D.B. Corry. 2020. Coronavirus vaccine-associated lung immunopathology-what is the significance? *Microbes Infect.* 22:403–404. https://doi.org/10.1016/j.micinf.2020.06.007

Bowyer, G., T. Rampling, J. Powlson, R. Morter, D. Wright, A.V.S. Hill, and K.J. Ewer. 2018. Activation-induced markers detect vaccine-specific $CD4^+$ T cell responses not measured by assays conventionally used in clinical trials. *Vaccines (Basel).* 6:50. https://doi.org/10.3390/vaccines6030050

Callendret, B., J. Vellinga, K. Wunderlich, A. Rodriguez, R. Steigerwald, U. Dirmeier, C. Cheminay, A. Volkmann, T. Brasel, R. Carrion, et al. 2018. A prophylactic multivalent vaccine against different filovirus species is immunogenic and provides protection from lethal infections with Ebolavirus and Marburgvirus species in non-human primates. *PLoS One.* 13:e0192312. https://doi.org/10.1371/journal.pone.0192312

Centers for Disease Control and Prevention. 2020. Coronavirus Disease 2019 (COVID-19). People at increased risk. https://www.cdc.gov/coronavirus/2019-ncov/need-extra-precautions/older-adults.html (accessed November 14, 2020).

Chen, Z., L. Zhang, C. Qin, L. Ba, C.E. Yi, F. Zhang, Q. Wei, T. He, W. Yu, J. Yu, et al. 2005. Recombinant modified vaccinia virus Ankara expressing the spike glycoprotein of severe acute respiratory syndrome coronavirus induces protective neutralizing antibodies primarily targeting the receptor binding region. *J. Virol.* 79:2678–2688. https://doi.org/10.1128/JVI.79.5.2678-2688.2005

Chen, H., Z. Xie, R. Long, S. Fan, H. Li, Z. He, K. Xu, Y. Liao, L. Wang, Y. Zhang, et al. 2020. A valid protective immune response elicited in rhesus macaques by an inactivated vaccine is capable of defending against SARS-CoV-2 infection. *bioRxiv.* https://doi.org/10.1101/2020.08.04.235747 (Preprint posted August 4, 2020)

Chi, X., R. Yan, J. Zhang, G. Zhang, Y. Zhang, M. Hao, Z. Zhang, P. Fan, Y. Dong, Y. Yang, et al. 2020. A neutralizing human antibody binds to the N-terminal domain of the Spike protein of SARS-CoV-2. *Science.* 369: 650–655. https://doi.org/10.1126/science.abc6952

Cohen, J. 2019. How long do vaccines last? The surprising answers may help protect people longer. *Science.* https://doi.org/10.1126/science.aax7364

Corbett, K.S., B. Flynn, K.E. Foulds, J.R. Francica, S. Boyoglu-Barnum, A.P. Werner, B. Flach, S. O'Connell, K.W. Bock, M. Minai, et al. 2020. Evaluation of the mRNA-1273 Vaccine against SARS-CoV-2 in Nonhuman Primates. *N. Engl. J. Med.* 383:1544–1555. https://doi.org/10.1056/NEJMoa2024671

Crooke, S.N., I.G. Ovsyannikova, G.A. Poland, and R.B. Kennedy. 2019. Immunosenescence and human vaccine immune responses. *Immun. Ageing.* 16:25. https://doi.org/10.1186/s12979-019-0164-9

Cucinotta, D., and M. Vanelli. 2020. WHO Declares COVID-19 a Pandemic. *Acta Biomed.* 91:157–160.

Dagotto, G., N.B. Mercado, D.R. Martinez, Y.J. Hou, J.P. Nkolola, R.H. Carnahan, J.E. Crowe Jr., R.S. Baric, and D.H. Barouch. 2021. Comparison of Subgenomic and Total RNA in SARS-CoV-2 Challenged Rhesus Macaques. *J. Virol.* 95:1–11. https://doi.org/10.1128/JVI.02370-20

European Centre for Disease Prevention and Control. 2020. Rapid increase of a SARS-CoV-2 variant with multiple spike protein mutations observed in the UK. https://www.ecdc.europa.eu/sites/default/files/documents/SARS-CoV-2-variant-multiple-spike-protein-mutations-United-Kingdom.pdf (accessed December 21, 2020)

Fontanet, A., B. Autran, B. Lina, M.P. Kieny, S.S.A. Karim, and D. Sridhar. 2021. SARS-CoV-2 variants and ending the COVID-19 pandemic. *Lancet.* 397:952–954. https://doi.org/10.1016/S0140-6736(21)00370-6

Geisbert, T.W., M. Bailey, L. Hensley, C. Asiedu, J. Geisbert, D. Stanley, A. Honko, J. Johnson, S. Mulangu, M.G. Pau, et al. 2011. Recombinant adenovirus serotype 26 (Ad26) and Ad35 vaccine vectors bypass immunity to Ad5 and protect nonhuman primates against ebolavirus challenge. *J. Virol.* 85:4222–4233. https://doi.org/10.1128/JVI.02407-10

Gustafson, C.E., C. Kim, C.M. Weyand, and J.J. Goronzy. 2020. Influence of immune aging on vaccine responses. *J. Allergy Clin. Immunol.* 145: 1309–1321. https://doi.org/10.1016/j.jaci.2020.03.017

Haynes, B.F., L. Corey, P. Fernandes, P.B. Gilbert, P.J. Hotez, S. Rao, M.R. Santos, H. Schuitemaker, M. Watson, and A. Arvin. 2020. Prospects for a safe COVID-19 vaccine. *Sci. Transl. Med.* 12:eabe0948. https://doi.org/10.1126/scitranslmed.abe0948

Hierholzer, J.C., and R.A. Killington. 1996. Virus isolation and quantitation. *In* Virology Methods Manual. B.W.J. Mahy, and H.O. Kangro, editors. Academic Press, San Diego., https://doi.org/10.1016/B978-012465330-6/50003-8

Hou, Y.J., S. Chiba, P. Halfmann, C. Ehre, M. Kuroda, K.H. Dinnon III, S.R. Leist, A. Schäfer, N. Nakajima, K. Takahashi, et al. 2020. SARS-CoV-2 D614G variant exhibits efficient replication ex vivo and transmission in vivo. *Science.* 370:1464–1468. https://doi.org/10.1126/science.abe8499

Ledford, H. 2021. J&J's one-shot COVID vaccine offers hope for faster protection. *Nature.* https://doi.org/10.1038/d41586-021-00119-7

Ledgerwood, J.E., K. Zephir, Z. Hu, C.J. Wei, L. Chang, M.E. Enama, C.S. Hendel, S. Sitar, R.T. Bailer, R.A. Koup, et al. VRC 310 Study Team. 2013. Prime-boost interval matters: a randomized phase 1 study to identify the minimum interval necessary to observe the H5 DNA influenza vaccine priming effect. *J. Infect. Dis.* 208:418–422. https://doi.org/10.1093/infdis/jit180

Lee, W.S., A.K. Wheatley, S.J. Kent, and B.J. DeKosky. 2020. Antibody-dependent enhancement and SARS-CoV-2 vaccines and therapies. *Nat. Microbiol.* 5:1185–1191. https://doi.org/10.1038/s41564-020-00789-5

Longworth, E., R. Borrow, D. Goldblatt, P. Balmer, M. Dawson, N. Andrews, E. Miller, and K. Cartwright. 2002. Avidity maturation following vaccination with a meningococcal recombinant hexavalent PorA OMV

vaccine in UK infants. *Vaccine*. 20:2592–2596. https://doi.org/10.1016/S0264-410X(02)00151-2

Mallapaty, S. 2020. The coronavirus is most deadly if you are older and male - new data reveal the risks. *Nature*. 585:16–17. https://doi.org/10.1038/d41586-020-02483-2

McMahan, K., J. Yu, N.B. Mercado, C. Loos, L.H. Tostanoski, A. Chandrashekar, J. Liu, L. Peter, C. Atyeo, A. Zhu, et al. 2021. Correlates of protection against SARS-CoV-2 in rhesus macaques. *Nature*. 590:630–634. https://doi.org/10.1038/s41586-020-03041-6

Mercado, N.B., R. Zahn, F. Wegmann, C. Loos, A. Chandrashekar, J. Yu, J. Liu, L. Peter, K. McMahan, L.H. Tostanoski, et al. 2020. Single-shot Ad26 vaccine protects against SARS-CoV-2 in rhesus macaques. *Nature*. 586:583–588. https://doi.org/10.1038/s41586-020-2607-z

Munster, V.J., F. Feldmann, B.N. Williamson, N. van Doremalen, L. Pérez-Pérez, J. Schulz, K. Meade-White, A. Okumura, J. Callison, B. Brumbaugh, et al. 2020. Respiratory disease and virus shedding in rhesus macaques inoculated with SARS-CoV-2. *bioRxiv*. https://doi.org/10.1101/2020.03.21.001628 (Preprint posted March 21, 2020)

Neerukonda, S.N., R. Vassell, R. Herrup, S. Liu, T. Wang, K. Takeda, Y. Yang, T.L. Lin, W. Wang, and C.D. Weiss. 2020. Establishment of a well-characterized SARS-CoV-2 lentiviral pseudovirus neutralization assay using 293T cells with stable expression of ACE2 and TMPRSS2. *bioRxiv*. https://doi.org/10.1101/2020.12.26.424442 (Preprint posted December 26, 2020)

Planas, D., T. Bruel, L. Grzelak, and F. Guivel-benhassine. 2021. Sensitivity of infectious SARS-CoV-2 B.1.1.7 and B.1.351 variants to neutralizing antibodies. *bioRxiv*. https://doi.org/10.1101/2021.02.12.430472 (Preprint posted February 12, 2021)

Plante, J.A., Y. Liu, J. Liu, H. Xia, B.A. Johnson, K.G. Lokugamage, X. Zhang, A.E. Muruato, J. Zou, C.R. Fontes-Garfias, et al. 2021. Spike mutation D614G alters SARS-CoV-2 fitness. *Nature*. 592:116–121. https://doi.org/10.1038/s41586-020-2895-3

Polack, F.P., S.J. Thomas, N. Kitchin, J. Absalon, A. Gurtman, S. Lockhart, J.L. Perez, G. Pérez Marc, E.D. Moreira, C. Zerbini, et al. C4591001 Clinical Trial Group. 2020. Safety and Efficacy of the BNT162b2 mRNA Covid-19 Vaccine. *N. Engl. J. Med.* 383:2603–2615. https://doi.org/10.1056/NEJMoa2034577

Pulendran, B., and R. Ahmed. 2011. Immunological mechanisms of vaccination. *Nat. Immunol.* 12:509–517. https://doi.org/10.1038/ni.2039

Roozendaal, R., J. Hendriks, T. van Effelterre, B. Spiessens, L. Dekking, L. Solforosi, D. Czapska-Casey, V. Bockstal, J. Stoop, D. Splinter, et al. 2020. Nonhuman primate to human immunobridging to infer the protective effect of an Ebola virus vaccine candidate. *NPJ Vaccines*. 5:112. https://doi.org/10.1038/s41541-020-00261-9

Sadoff, J., M. Le Gars, G. Shukarev, D. Heerwegh, C. Truyers, A.M. de Groot, J. Stoop, S. Tete, W. Van Damme, I. Leroux-Roels, et al. 2021. Safety and immunogenicity of the Ad26.COV2.S COVID-19 vaccine candidate: interim results of a phase 1/2a, double-blind, randomized, placebo-controlled trial. *N. Engl. J. Med.* https://doi.org/10.1056/NEJMoa2034201

Salisch, N.C., A. Izquierdo Gil, D.N. Czapska-Casey, L. Vorthoren, J. Serroyen, J. Tolboom, E. Saeland, H. Schuitemaker, and R.C. Zahn. 2019. Adenovectors encoding RSV-F protein induce durable and mucosal immunity in macaques after two intramuscular administrations. *NPJ Vaccines*. 4:54. https://doi.org/10.1038/s41541-019-0150-4

Salisch, N.C., K.E. Stephenson, K. Williams, F. Cox, L. van der Fits, D. Heerwegh, C. Truyers, M.N. Habets, D.G. Kanjilal, R.A. Larocca, et al. 2021. A Double-Blind, Randomized, Placebo-Controlled Phase 1 Study of Ad26.ZIKV.001, an Ad26-Vectored Anti-Zika Virus Vaccine. *Ann. Intern. Med.*:M20-5306. https://doi.org/10.7326/M20-5306

Sallusto, F., A. Lanzavecchia, K. Araki, and R. Ahmed. 2010. From vaccines to memory and back. *Immunity*. 33:451–463. https://doi.org/10.1016/j.immuni.2010.10.008

Sanders, B.P., D. Edo-Matas, J.H.H.V. Custers, M.H. Koldijk, V. Klaren, M. Turk, A. Luitjens, W.A.M. Bakker, F. Uytdehaag, J. Goudsmit, et al. 2013. PER.C6(®) cells as a serum-free suspension cell platform for the production of high titer poliovirus: a potential low cost of goods option for world supply of inactivated poliovirus vaccine. *Vaccine*. 31:850–856. https://doi.org/10.1016/j.vaccine.2012.10.070

Shan, C., Y.F. Yao, X.L. Yang, Y.W. Zhou, G. Gao, Y. Peng, L. Yang, X. Hu, J. Xiong, R.D. Jiang, et al. 2020. Infection with novel coronavirus (SARS-CoV-2) causes pneumonia in Rhesus macaques. *Cell Res.* 30:670–677. https://doi.org/10.1038/s41422-020-0364-z

Siegrist, C.-A. 2018. Vaccine immunology. *In* Plotkin's Vaccines. S.A. Plotkin, W.A. Orenstein, P.A. Offit, and K.M. Edwards, editors. Elsevier, Philadelphia. pp. 16–34.e7., https://doi.org/10.1016/B978-0-323-35761-6.00002-X

Tegally, H., E. Wilkinson, M. Giovanetti, A. Iranzadeh, V. Fonseca, J. Giandhari, D. Doolabh, S. Pillay, E.J. San, N. Msomi, et al. 2020. Emergence and rapid spread of a new severe acute respiratory syndrome-related coronavirus 2 (SARS-CoV-2) lineage with multiple spike mutations in South Africa. *medRxiv*. https://doi.org/10.1101/2020.12.21.20248640 (Preprint posted December 22, 2020)

Thomson, E.C., L.E. Rosen, J.G. Shepherd, R. Spreafico, S. Filipe, J.A. Wojcechowskyj, C. Davis, L. Piccoli, D.J. Pascall, J. Dillen, et al. 2020. The circulating SARS-CoV-2 spike variant N439K maintains fitness while evading antibody-mediated immunity. *bioRxiv*. https://doi.org/10.1101/2020.11.04.355842 (Preprint posted November 5, 2020)

Tostanoski, L.H., F. Wegmann, A.J. Martinot, C. Loos, K. McMahan, N.B. Mercado, J. Yu, C.N. Chan, S. Bondoc, C.E. Starke, et al. 2020. Ad26 vaccine protects against SARS-CoV-2 severe clinical disease in hamsters. *Nat. Med.* 26:1694–1700. https://doi.org/10.1038/s41591-020-1070-6

van Doremalen, N., T. Lambe, A. Spencer, S. Belij-Rammerstorfer, J.N. Purushotham, J.R. Port, V.A. Avanzato, T. Bushmaker, A. Flaxman, M. Ulaszewska, et al. 2020. ChAdOx1 nCoV-19 vaccine prevents SARS-CoV-2 pneumonia in rhesus macaques. *Nature*. 586:578–582. https://doi.org/10.1038/s41586-020-2608-y

Victora, G.D., and M.C. Nussenzweig. 2012. Germinal centers. *Annu. Rev. Immunol.* 30:429–457. https://doi.org/10.1146/annurev-immunol-020711-075032

Vogel, A., I. Kanevsky, Y. Che, K. Swanson, A. Muik, M. Vormehr, L. Kranz, K. Walzer, S. Hein, A. Gueler, et al. 2020. A prefusion SARS-CoV-2 spike RNA vaccine is highly immunogenic and prevents lung infection in non-human primates. *bioRxiv*. https://doi.org/10.1101/2020.09.08.280818 (Preprint posted September 8, 2020)

Voysey, M., S.A.C. Clemens, S.A. Madhi, L.Y. Weckx, P.M. Folegatti, P.K. Aley, B. Angus, V.L. Baillie, S.L. Barnabas, Q.E. Bhorat, et al. Oxford COVID Vaccine Trial Group. 2021. Safety and efficacy of the ChAdOx1 nCoV-19 vaccine (AZD1222) against SARS-CoV-2: an interim analysis of four randomised controlled trials in Brazil, South Africa, and the UK. *Lancet*. 397:99–111. https://doi.org/10.1016/S0140-6736(20)32661-1

Wagner, A., E. Garner-Spitzer, J. Jasinska, H. Kollaritsch, K. Stiasny, M. Kundi, and U. Wiedermann. 2018. Age-related differences in humoral and cellular immune responses after primary immunisation: indications for stratified vaccination schedules. *Sci. Rep.* 8:9825. https://doi.org/10.1038/s41598-018-28111-8

Wang, H., Y. Zhang, B. Huang, W. Deng, Y. Quan, W. Wang, W. Xu, Y. Zhao, N. Li, J. Zhang, et al. 2020. Development of an Inactivated Vaccine Candidate, BBIBP-CorV, with Potent Protection against SARS-CoV-2. *Cell*. 182:713–721.e9. https://doi.org/10.1016/j.cell.2020.06.008

Weinberger, B. 2018. Vaccines for the elderly: current use and future challenges. *Immun. Ageing*. 15:3. https://doi.org/10.1186/s12979-017-0107-2

Weissman, D., M.-G. Alameh, T. de Silva, P. Collini, H. Hornsby, R. Brown, C.C. LaBranche, R.J. Edwards, L. Sutherland, S. Santra, et al. 2021. D614G Spike Mutation Increases SARS CoV-2 Susceptibility to Neutralization. *Cell Host Microbe*. 29:23–31.e4. https://doi.org/10.1016/j.chom.2020.11.012

Wölfel, R., V.M. Corman, W. Guggemos, M. Seilmaier, S. Zange, M.A. Müller, D. Niemeyer, T.C. Jones, P. Vollmar, C. Rothe, et al. 2020. Virological assessment of hospitalized patients with COVID-2019. *Nature*. 581:465–469. https://doi.org/10.1038/s41586-020-2196-x

World Health Organization. 2020a. SARS-CoV-2 Variants. WHO Disease Outbreak News 31 December 2020. https://www.who.int/csr/don/31-december-2020-sars-cov2-variants/en/ (accessed February 14, 2021)

World Health Organization. 2020b. Weekly operational update on COVID-19: 23 October 2020. https://www.who.int/publications/m/item/weekly-update-on-covid-19—23-october (accessed October 23, 2020).

Wu, F., S. Zhao, B. Yu, Y.M. Chen, W. Wang, Z.G. Song, Y. Hu, Z.W. Tao, J.H. Tian, Y.Y. Pei, et al. 2020. A new coronavirus associated with human respiratory disease in China. *Nature*. 579:265–269. https://doi.org/10.1038/s41586-020-2008-3

Wu, K., A.P. Werner, J.I. Moliva, M. Koch, A. Choi, G.B.E. Stewart-Jones, H. Bennett, S. Boyoglu-Barnum, W. Shi, B.S. Graham, et al. 2021. mRNA-1273 vaccine induces neutralizing antibodies against spike mutants from global SARS-CoV-2 variants. *bioRxiv*. https://doi.org/10.1101/2021.01.25.427948 (Preprint posted January 25, 2021)

Wunderlich, K., T.G. Uil, J. Vellinga, B.P. Sanders, and R. Van der Vlugt. 2018. Potent And Short Promoter For Expression Of Heterologous Genes. US Patent No. US-2018223314-A1, filed February 8, 2018, publication date of the patent application August 9, 2018.

Xie, X., Y. Liu, J. Liu, X. Zhang, J. Zou, C. R. Fontes-Garfias, H. Xia, K. A. Swanson, M. Cutler, D. Cooper, et al. 2021. Neutralization of SARS-CoV-2 spike 69/70 deletion, E484K and N501Y variants by BNT162b2 vaccine-elicited sera. *Nat. Med.* 27:620–621. https://doi.org/10.1038/s41591-021-01270-4

Yu, J., L.H. Tostanoski, L. Peter, N.B. Mercado, K. McMahan, S.H. Mahrokhian, J.P. Nkolola, J. Liu, Z. Li, A. Chandrashekar, et al. 2020. DNA vaccine protection against SARS-CoV-2 in rhesus macaques. *Science.* 369:806–811. https://doi.org/10.1126/science.abc6284

Zahn, R., G. Gillisen, A. Roos, M. Koning, E. van der Helm, D. Spek, M. Weijtens, M. Grazia Pau, K. Radošević, G.J. Weverling, et al. 2012. Ad35 and ad26 vaccine vectors induce potent and cross-reactive antibody and T-cell responses to multiple filovirus species. *PLoS One.* 7:e44115. https://doi.org/10.1371/journal.pone.0044115

Zhu, N., D. Zhang, W. Wang, X. Li, B. Yang, J. Song, X. Zhao, B. Huang, W. Shi, R. Lu, et al. China Novel Coronavirus Investigating and Research Team. 2020. A novel coronavirus from patients with pneumonia in China, 2019. *N. Engl. J. Med.* 382:727–733. https://doi.org/10.1056/NEJMoa2001017

Zimmermann, P., and N. Curtis. 2019. Factors That Influence the Immune Response to Vaccination. *Clin. Microbiol. Rev.* 32:e00084-18. https://doi.org/10.1128/CMR.00084-18

Supplemental material

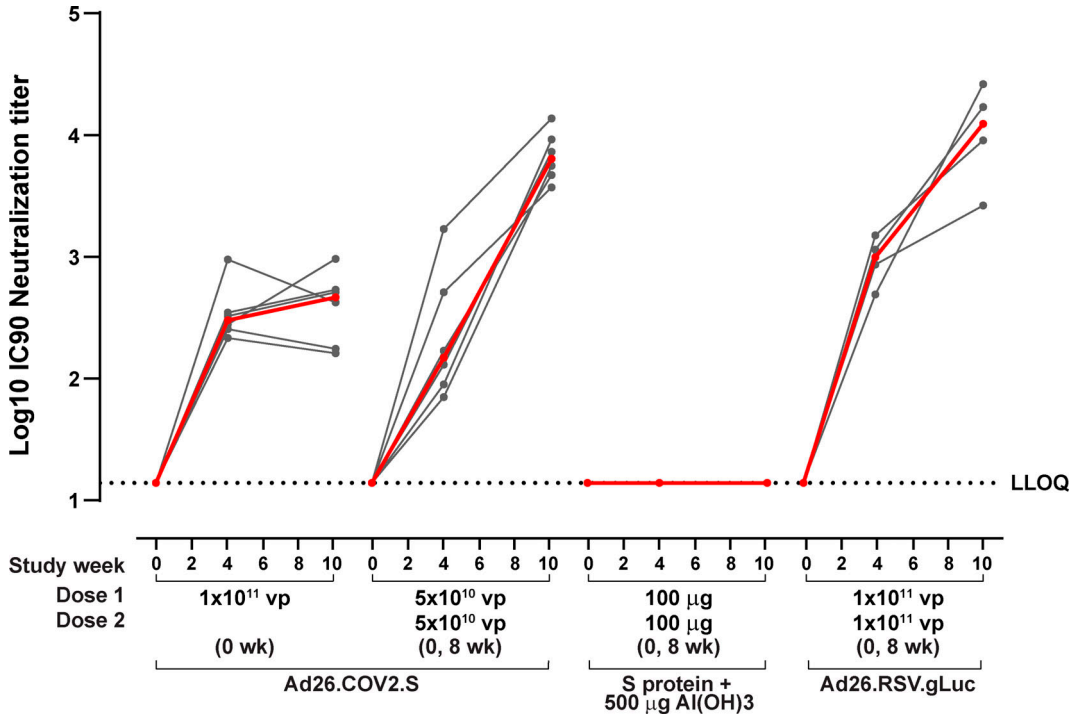

Figure S1. **Ad26 neutralizing antibodies measured in 20 NHPs at indicated time points (three time points, week 0, week 4, and week 10).** Antibody levels in the individual animals are depicted with gray points, and paired measurements are connected with gray lines. The geometric mean titer of neutralizing antibody responses per group is indicated with the red line. The dotted lines indicate the LLOQ.

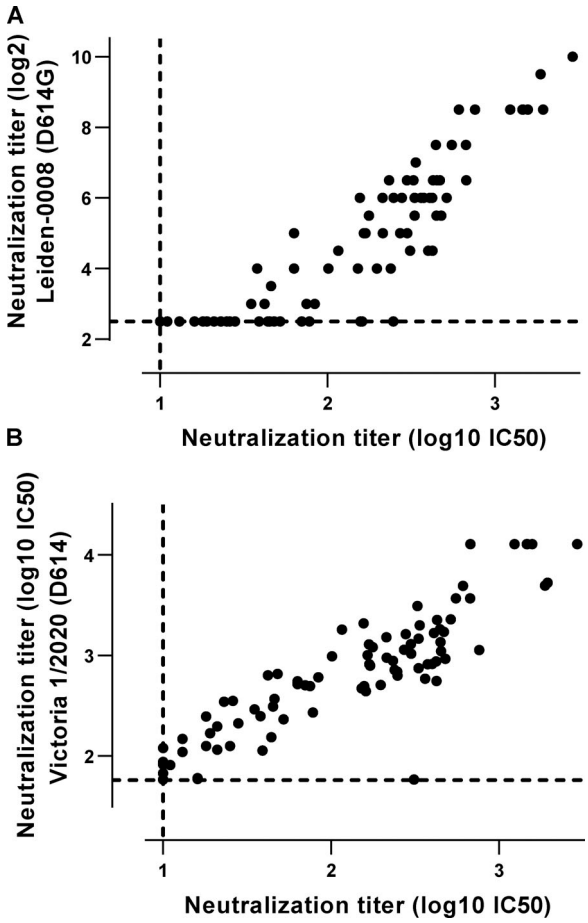

Figure S2. **Correlation between SARS-CoV-2 neutralizing antibody titers as measured by different VNA assays for all groups and time points except week 0 time point. (A)** Correlation between Leiden-0008 strain (B.1 lineage; LUMC) and Wuhan-Hu-1 (A lineage, Nexelis). r_s = 0.90, P < 0.001. **(B)** Correlation between the Victoria/1/202 strain (A lineage; PHE) and Wuhan-Hu-1 (A lineage, Nexelis). r_s = 0.91, P < 0.001. The dotted lines indicate the LLOD for each assay. Correlation coefficients between different neutralization assays were calculated using two-sided Spearman rank correlation.

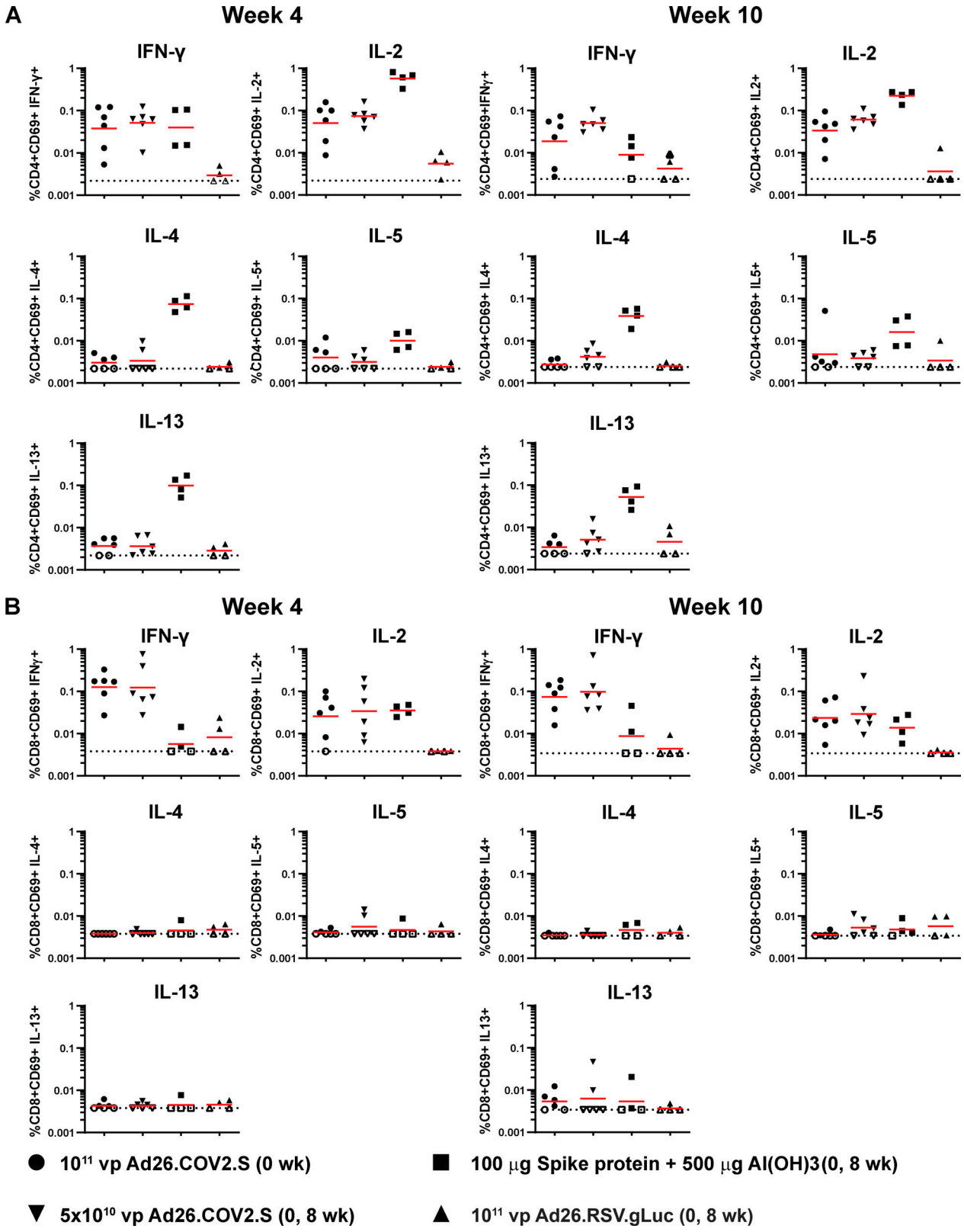

Figure S3. **Spike protein–specific CD4 and CD8 T cell responses after vaccination of aged rhesus macaques. (A)** Spike protein–specific T cell responses as measured in 40 NHP PBMC samples (20 NHPs and two time points) by ICS at indicated time points. Frequency of $CD4^+CD69^+$ T cell–expressing cytokines. The geometric mean response per group is indicated with a horizontal line. The dotted line indicates the technical threshold. Open symbols denote samples at technical threshold. **(B)** Spike (S) protein–specific T cell responses as measured by ICS at indicated time points. Frequency of $CD8^+CD69^+$ T cell–expressing cytokines. The geometric mean response per group is indicated with a horizontal line. The dotted line indicates the technical threshold. Open symbols denote samples at technical threshold.

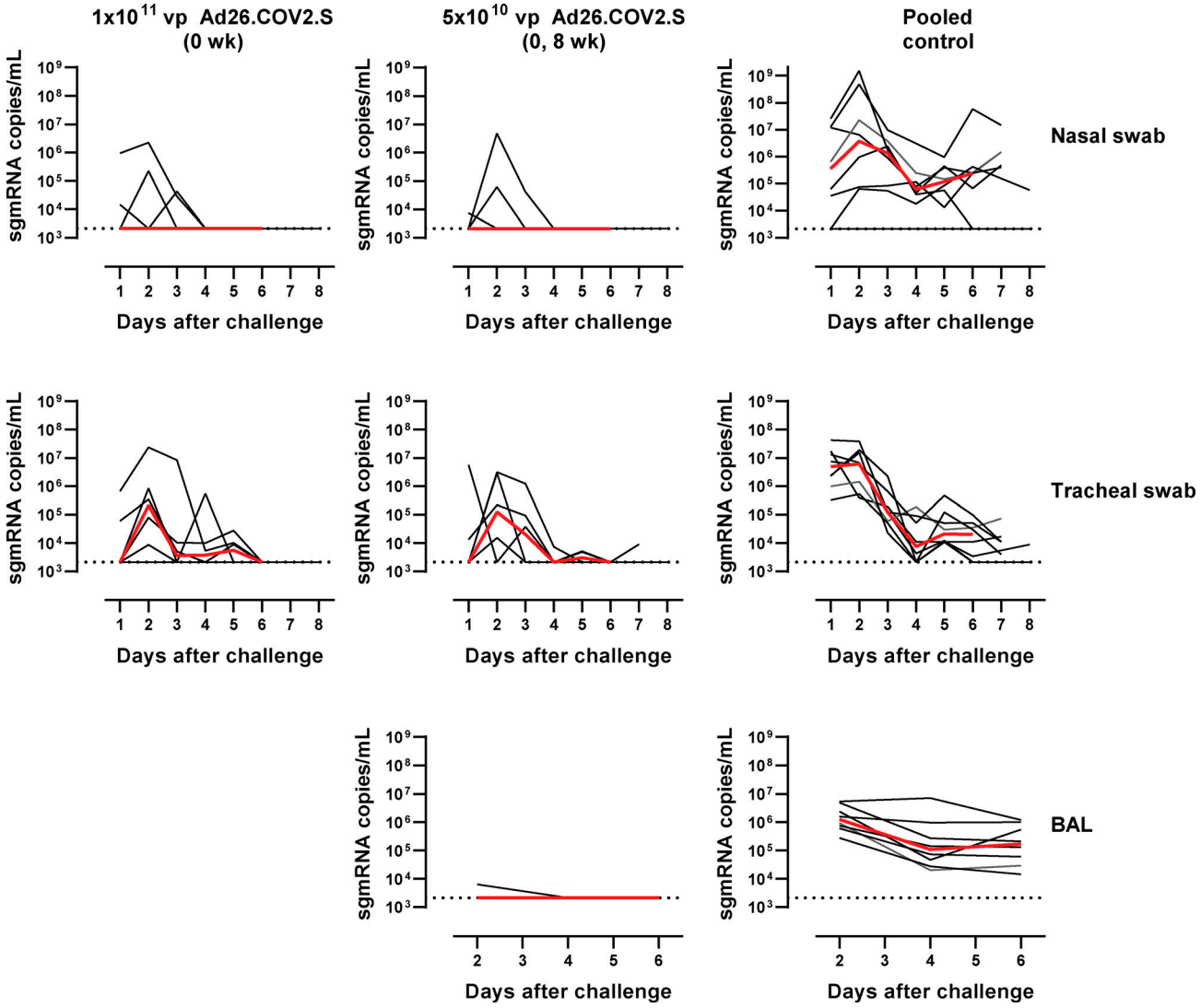

Figure S4. **Viral load (sgmRNA copies/ml) kinetics in swabs and BAL after SARS-CoV-2 inoculation of 19 vaccinated aged rhesus macaques.** Black lines represent individual animals, red lines the group median up to day 6, the last day of follow-up before scheduled euthanasia. Dotted horizontal line represents the LLOQ. Data of a related challenge of naive animals (n = 4) using an identical challenge strain, challenge regimen, and readouts were added to the sham control group data, collectively referred to as pooled control, to increase statistical power.

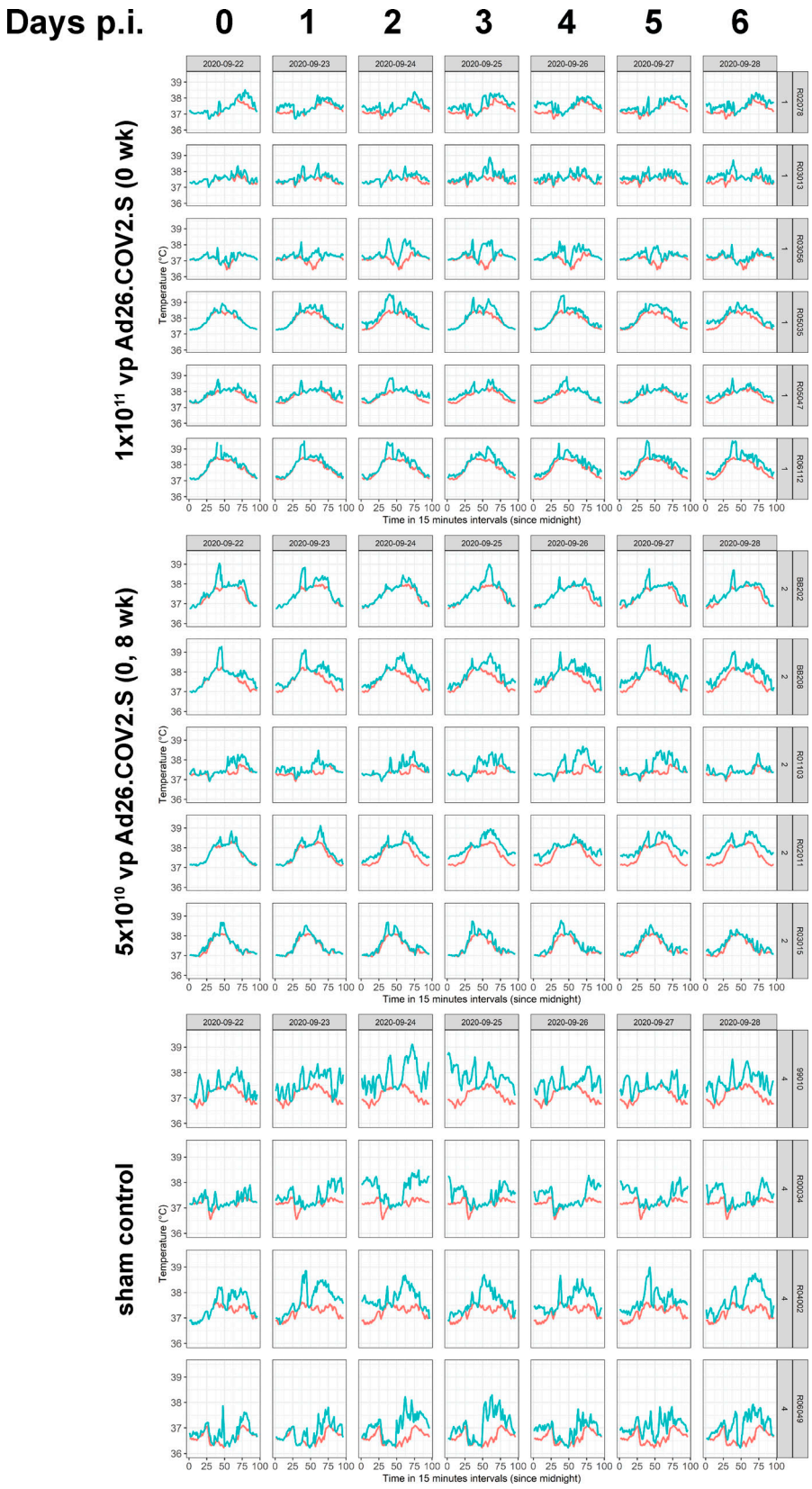

Figure S5. **Body temperatures after SARS-CoV-2 inoculation of 19 vaccinated aged rhesus macaques on day of infection and for 6 consecutive d afterward.** Calendar dates are on top, animal id and group number labels on the right-hand side. Orange lines indicate the daily baseline temperature profile derived from a multiday window before virus inoculation in which no biotechnical interventions occurred. The blue line is the temperature of each animal after infection. Top: Body temperatures of the 10^{11}-vp Ad26.COV2.S group. Middle: Body temperatures of the 5×10^{10}–vp Ad26.COV2.S group. Bottom: Body temperatures of the pooled control animal group. p.i., post infection.